

Aus der Abteilung für Klinische Pharmakologie

Direktor: Prof. Dr. med. S. Endres

Medizinische Klinik und Poliklinik IV

Klinikum der Universität

Ludwig-Maximilians-Universität München

Direktor: Prof. Dr. med. M. Reincke

**Engineering model antigen-specific T cells to overexpress the chemokine receptor
CXCR6 improves homing of adoptively transferred T cells in
subcutaneous tumor models**

Dissertation

zum Erwerb des Doctor of Philosophy (Ph. D.)

an der Medizinischen Fakultät der

Ludwig-Maximilians-Universität München

vorgelegt von

Stefanie Lesch

aus Marburg-Wehrda

21.05.2019

Mit Genehmigung der Medizinischen Fakultät
der Universität München

Prüfer 1:

Prof. Dr. med. Sebastian Kobold

Prüfer 2:

Prof. Dr. rer. nat. Karl-Peter Hopfner

Prüfer 3:

Prof. Dr. rer. nat. Wolfgang Alois Zimmermann

Prüfer 4:

Prof. Dr. med. Stefan Endres

Dekan:

Prof. Dr. med. Reinhard HICKEL

Tag der mündlichen Prüfung:

15.10.2019

Table of content

1	Introduction	1
1.1	The importance of the immune system in cancer development and progression.....	1
1.2	Cancer immunotherapy	2
1.2.1	Adoptive cell therapy (ACT).....	2
1.2.2	Chimeric antigen receptor (CAR)-engineered T cells for cancer immunotherapy	3
1.2.3	Limitations of ACT and improvement strategies to increase the susceptibility of solid tumors to CAR T cell therapy	4
1.3	Chemokines and chemokine receptors	5
1.3.1	The role of chemokines in tumors	6
1.3.2	Arming tumor-specific T cells with chemokine receptors to improve ACT.....	7
1.3.3	The CXCL16-CXCR6 axis	8
1.4	Research objectives	9
2	Materials	11
2.1	Technical equipment	11
2.2	Materials	11
2.3	Chemicals and reagents.....	12
2.4	Cytokines.....	13
2.5	Antibodies.....	13
2.6	Kits and assays	13
2.7	Cell lines, supplements and media.....	14
2.7.1	Cell lines	14
2.7.2	Supplements.....	15
2.7.3	Media.....	15
2.7.4	Buffers	16
2.8	Software	16
3	Methods	17
3.1	Molecular biological methods	17
3.1.1	Generation of plasmids for retrovirus-mediated gene transfer	17
3.1.2	RNA isolation and quantitative real-time PCR (qRT-PCR).....	17
3.2	Cell biological methods.....	17
3.2.1	General cell culture conditions	17
3.2.2	Generation of cell-free tumor supernatants	18
3.2.3	Isolation of primary murine T cells.....	18

3.2.4	Isolation of primary human T cells.....	19
3.2.5	Retroviral transduction of murine T cells	19
3.2.6	Retroviral transduction of human T cells	20
3.2.7	Isolation of cells from organs.....	20
3.2.8	Generation of organ lysates	20
3.2.9	Confocal microscopy assay.....	21
3.2.10	Cell adhesion assay	21
3.2.11	Migration and spheroid invasion assay	21
3.2.12	T cell stimulation and cytotoxicity assays	22
3.3	Immunological methods.....	22
3.3.1	Enzyme-linked immunosorbent assay (ELISA)	22
3.3.2	Flow cytometry analysis (FACS)	22
3.4	Animal experiments	23
3.4.1	Care of laboratory animals	23
3.4.2	Subcutaneous tumor models.....	23
3.5	Statistical analysis	24
4	Results.....	25
4.1	Expression of CXCL16 and its receptor CXCR6 in a murine model.....	25
4.1.1	<i>In vitro</i> expression of the chemokine CXCL16 in murine tumor models.....	25
4.1.2	CXCL16 is expressed by tumor-infiltrating CD11c-positive myeloid cells	26
4.1.3	Genetic modification of murine cytotoxic T cells with CXCR6	27
4.2	<i>In vitro</i> characterization of CXCR6-transduced T cells.....	27
4.2.1	CXCR6 mediates migration of primary murine T cells.....	27
4.2.2	CXCR6 internalization and recycling upon CXCL16 engagement	28
4.2.3	CXCR6 enhances recognition of CXCL16-producing tumor cells	29
4.2.4	CXCR6 facilitates T cell adhesion to a CXCL16-positive surface	30
4.3	<i>In vivo</i> characterization of CXCR6-transduced OT-1 T cells	31
4.3.1	CXCR6 specifically improves the antitumor efficiency of adoptively transferred OT-1 T cells shown by delayed tumor growth <i>in vivo</i>	31
4.3.2	CXCR6 mediates T cell homing to tumor tissue	33
4.4	Expression of CXCL16 and its receptor CXCR6 in a human model.....	35
4.4.1	<i>In vitro</i> expression of the chemokine CXCL16 in human tumor models.....	35
4.4.2	Genetic modification of human cytotoxic T cells with a CXCR6-encoding retroviral vector.....	36
4.4.3	hCXCR6 enables human T cells to migrate towards hCXCL16 gradients	37
4.4.4	hCXCR6 mediates penetration of T cells into 3D tumor spheroids	38

5	Discussion	40
5.1	IFN- γ amplifies the expression of CXCL16 by tumor cells	40
5.2	CXCR6-mediated migration and adhesion improved target cell lysis by tumor-specific T cells <i>in vitro</i>	41
5.3	CXCR6 improves the anti-tumoral effects of ACT	43
5.4	CXCR6-mediated therapeutic effects are dependent on a sufficient chemokine gradient	44
5.5	CXCR6 ameliorates T cell homing into tumor tissue	45
5.6	CXCR6 enables human primary T cells to migrate towards CXCL16 gradients and invade tumor spheroids	47
5.7	Conclusion and perspective	48
6	Summary	51
7	Reference list	52
8	Appendices	63
8.1	Abbreviations	63
8.2	Publications	65

1 Introduction

1.1 The importance of the immune system in cancer development and progression

The complex and dynamic acquisition of malignant properties in normal cells is known as tumorigenesis. The hallmarks of cancer comprise main characteristics associated with this process, such as an increased proliferation, evasion of apoptosis and escape from immunosurveillance (Hanahan et al., 2011). Numerous studies have identified a high rate of somatic gene mutations in classical oncogenes or tumor suppressor genes causing malignant transformation of normal cells (Alexandrov et al., 2013). However, tumor formation can only occur if the tissue environment provides a milieu that can sustain tumor growth and progression. A complex bidirectional interaction takes place between the genetically unstable malignant cells and the surrounding milieu. This interaction determines important tumor properties such as tumor promotion and proliferation, invasiveness, metastasis and thus also influences the patients' prognosis. Therefore, the tumor microenvironment (TME), including non-malignant cells, cytokines, growth factors as well as inflammatory and matrix remodeling enzymes, plays a crucial role in tumorigenesis (Joyce et al., 2009; Balkwill et al., 2012; Hanahan et al., 2012).

Immunosurveillance describes the elimination of senescent, damaged or malignant cells by the immune system and functions as a major mechanism in maintaining tissue integrity. Defects in molecular or cellular components involved in this immune response lead to tumor progression and metastasis (Joyce et al., 2009). The immune response against malignant cells during the process of tumor growth is subdivided into three stages: elimination, equilibrium, and escape. In the first stage, immune cells recognize and eliminate tumor cells due to the expression of tumor antigens, thus protecting the host against cancer. The next stage is a dynamic equilibrium between tumor and immune cells since the immune system is incapable to completely destroy the neoplastic lesion. Following equilibrium, the malignant cells acquire the probability to escape the immune system leading to tumor formation (Mittal et al., 2014). Many studies illustrate mechanisms suppressing an effective immunosurveillance including the secretion of immunoregulatory proteins such as transforming growth factor (TGF)- β or the tumoral expression of checkpoint molecules such as programmed cell death protein 1 (PD-1) and cytotoxic T lymphocyte antigen 4 (CTLA-4) (Gorelik et al., 2001; Pardoll, 2012). In addition, the recruitment of regulatory T (Treg) cells and myeloid-derived suppressor cells (MDSCs) by the tumor tissue is diminishing the immune response (Rabinovich et al., 2007). All of this can be an explanation for the poor immunogenicity of most clinically relevant tumors.

Established standard therapies for cancer patients are surgical resection, chemotherapy and irradiation, and more recently immunotherapy. The aim of cancer immunotherapy is to harness the patient's immune system to induce tumor control and rejection.

1.2 Cancer immunotherapy

In the recent years, several approaches to activate the immune system against cancer including immunostimulatory agents, monoclonal antibodies, cancer vaccines, and cell-based therapies have been developed. Therapeutic strategies that focus on inhibitory signals received by T cells, including monoclonal antibodies targeting CTLA-4 (ipilimumab) and PD-1 (nivolumab) have been developed. For example in melanoma patients, these strategies led to enhanced overall survival (Eggermont et al., 2016; Topalian et al., 2014). Thus in 2011, the U. S. Food and Drug Administration (FDA) approved ipilimumab for the treatment of melanoma whereas nivolumab obtained approval for a growing number of tumor entities since 2014 (www.fda.gov). More recently the combination of both antibodies has shown promising responses in patients with intermediate or poor-risk advanced renal cell carcinoma (NCT02231749) resulting in the FDA approval of nivolumab plus ipilimumab for the treatment of this malignancy (www.fda.gov).

Studies examining different tumor entities describe a positive correlation between immune cell infiltrates and an improved prognosis due to an increased anti-tumor response (Schaer et al., 2011; Geng et al., 2015). Tumor-specific T cells are able to recognize tumor antigen-expressing antigen-presenting cells (APC) or tumor cells themselves. After tumor antigen engagement, T cells can directly mediate cytotoxic responses against cancer cells, either through the release of cytotoxic granules or through the expression of apoptosis-inducing molecules (Restifo et al., 2012). Activated CD8⁺ T cells are capable of releasing pro-inflammatory cytokines such as interferon (IFN)- γ to enhance the immune response. The counterparts of tumor-infiltrating lymphocytes (TILs) are Treg cells, which compromise the protective features of TILs by hampering their activation and proliferation (Ganesan et al., 2013). Therefore, increasing the access of therapeutic TILs to tumors in order to shift the balance towards effector T cells and the maintenance of their activity are promising options to enhance anti-tumor response. This can be achieved by adoptive cell therapy (ACT).

1.2.1 Adoptive cell therapy (ACT)

In the field of cancer immunotherapy the transfer of autologous T cells, isolated from tumor biopsies and expanded *ex vivo*, has emerged as a powerful therapeutic strategy for the treatment of patients with advanced malignancies (Kalos et al., 2013). However, only 30 to 40 % of tumor biopsies contain sufficient numbers of TILs (Dudley et al., 2003).

Therefore, autologous T cells from peripheral blood transduced with high-affinity tumor antigen-specific T cell receptors (TCRs) or chimeric antigen receptors (CARs) are the most explored avenues, due to their more generic basis.

1.2.2 Chimeric antigen receptor (CAR)-engineered T cells for cancer immunotherapy

The adoptive transfer of T cells, which have been engineered to express an artificial CAR targeting a specific antigen expressed on the surface of tumor cells is a promising approach for cancer immunotherapy. Over the last decade, adoptive transfer of *ex vivo* modified and expanded CAR T cells has been shown to be an effective treatment for hematological malignancies (Park et al., 2016). As a result, the FDA approved the first two CAR T cell therapies (Kymriah™ and Yescarta™) for the treatment of relapsed and refractory B cell acute lymphoblastic leukemia (ALL) or large B cell lymphoma positive for the CD19 antigen in 2017 (www.fda.gov).

Initially, CAR constructs were cell surface proteins consisting of the V_H and V_L regions of a tumor antigen-specific monoclonal antibody expressed as a single chain variable fragment (scFv), which was linked to a signal transduction domain of the CD3ζ chain (Stancovski et al., 1993). Clinical trials using such first generation CAR constructs were not able to initiate an effective *in vivo* anti-tumor activity (Kershaw et al., 2006). Thereafter, CAR constructs were designed with one or more additional co-stimulatory domains to enhance cytokine production and proliferation of engineered T cells. So-called second or third generation CAR constructs incorporating CD3ζ fused to CD28, 4-1BB or OX40 revealed a superior anti-tumor efficiency compared to first generation CAR constructs (Wang et al., 2007; Hombach et al., 2013).

In comparison to TCR-transduced T cells, CAR-mediated ACT has several advantages, including HLA-independent tumor antigen recognition. The activation of TCR-transduced T cells is limited by the presentation of tumor antigens on HLA molecules on the tumor cells. Thus a described mechanism of immune evasion is the down-regulation of HLA molecules (Garrido et al., 2016). Another advantage is the possibility to link additional signaling modules to one antigen recognition domain resulting in optimal activation, proliferation and cytokine secretion by the engineered T cells (June, 2007).

Because of the impressive benefits in the treatment of hematologic malignancies, the values of CAR T cell therapy were also investigated for solid tumors, such as breast cancer, sarcoma, neuroblastoma and others (Bajgain et al., 2018; Ahmed et al., 2015; Prapa et al., 2015). However, these approaches led to less encouraging results probably due to the more

complex composition of solid tumors, heterogeneous tumor antigen expression as well as the immunosuppressive effects of the TME.

1.2.3 Limitations of ACT and improvement strategies to increase the susceptibility of solid tumors to CAR T cell therapy

ACT has an enormous potential for the treatment of hematological malignancies. But so far, the success of ACT in the treatment of solid tumors is limited due to immunosuppressive mechanisms at the tumor site. Here the presence of Treg cells and MDSCs, as well as metabolic conditions inhibit the activation of cytotoxic T cells after tumor infiltration (Balkwill et al., 2012). Additionally, tumor cells themselves are able to directly suppress effector T cell function. For instance, programmed cell death ligand 1 (PD-L1) is a negative regulator of T cell effector function and is frequently expressed in solid tumors (Pardoll, 2012). After activation, T cells up-regulate PD-1 and the interaction with PD-L1 on the tumor cell surface leads to functionally exhausted T cells. In our group, a strategy has been designed to convert this inhibitory signal in a T cell activation signal by exchanging the intracellular signaling domain of PD-1 with that of CD28. T cells expressing this fusion receptor become activated rather than exhausted upon PD-L1 engagement. Therefore, this receptor serves as a promising strategy to overcome PD-L1-mediated immunosuppression (Kobold et al., 2015; Liu et al., 2016; Rataj et al., 2018). However, not all tumor entities are susceptible to PD-1-PD-L1 engagement. Therefore, further innovative approaches are required to bypass immunosuppressive hurdles, maintain effector functions and facilitate an efficient anti-tumor attack by the transferred T cell.

In addition, only a limited number of tumor-specific antigens that are ubiquitously expressed on tumor cells but not on healthy tissue have been identified. Currently, molecules with higher expression levels on tumor cells compared to healthy tissue have been selected as potential targets but might have safety concerns. Targeting molecules whose expression is not restricted to solid tumors carries the risk to damage healthy tissue due to on-target off-tumor toxicity. Therefore, a major research objective in the area of cancer immunotherapy is the identification of tumor-specific antigens (TSA) for the design of novel CAR constructs to improve CAR T cell specificity and safety.

In some patients significant and partially life-threatening toxicity due to synchronous CAR T cell activation and effector cytokine production has been observed (Morgan et al., 2010). This situation in which CAR T cells are activated tumor-independently (on-target/off-tumor toxicity) is described as cytokine storm (Porter et al., 2018). This underlines the importance of safety mechanism to ameliorate CAR T cell therapy. To regulate the cytotoxic effects of

transferred T cells in patients and to minimize the magnitude of adverse effects, CAR T cells can be additionally engineered with suicide genes. Several suicide genes are currently tested in CAR-engineered T cells, such as the inducible caspase-9-based suicide gene (iCasp9), which enables a rapid and sufficient elimination of CAR T cells after activation (Hoyos et al., 2010).

Tumor escape from CAR T cell therapy can occur due to the down-regulation of targeted tumor antigens and subsequent selective outgrowth of antigen-negative variants. Simultaneous targeting of two different tumor antigens might overcome this hurdle. Therefore, two ligand binding domains separated by a linker or T cells engineered to express different CAR constructs could be used (Grada et al., 2013).

The efficiency of ACT relies on the cytotoxic properties of transferred CAR T cells, but the importance of an efficient homing of the effector T cells to the target site should not be underestimated. To fulfill their therapeutic effects, adoptively transferred engineered T cells have to traffic in a sufficient quantity to the tumor site. The homing of T cells is a complex multistep process that includes exiting the circulation and infiltrating the tumor mediated by chemokines secreted by the tumor milieu (Fisher et al., 2006). Improvements can be made to ameliorate these essential steps of ACT. One strategy to enhance ACT for the treatment of solid tumors is to increase the trafficking of immune effector cells into the tumor through the genetic introduction of chemokine receptors. The expression of one or multiple chemokine receptors, depending on the chemokine profile of the tumor, could directly mediate a specific migration of cytotoxic T cells to the tumor site (Di Stasi et al., 2009).

1.3 Chemokines and chemokine receptors

Chemokines are a family of small proteins (8-10 kDa) that exhibit structural similarity with each other and are classified into the four subfamilies CXC, CC, C and CX3C, based on the configuration of their amino-terminal cysteine residues (Zlotnik et al., 2000). Chemokines are known for their capability to regulate the recruitment and trafficking of cells through chemoattraction. In physiological situations or by infection or inflammation, chemokines orchestrate homeostatic trafficking of several cell types such as hematopoietic stem cells, lymphocytes, monocytes, and dendritic cells. In addition, the small chemoattractants play a crucial role in diverse processes, including the development of the nervous system, homeostatic trafficking of hematopoietic stem cells, lymphocytes and dendritic cells (Raman et al., 2011). Chemokines exert their function by interaction with G protein-coupled receptors, also known as seven-transmembrane domain receptors. Binding to the extracellular amino-terminal region of the appropriate receptor leads to phosphorylation of serine and threonine

residues in the intracellular carboxy-terminal region and activation of a signaling cascade culminating in the transcription of genes involved in invasion, motility, extracellular matrix interaction and cell survival (Neel et al., 2005). To date, more than 50 different chemokines have been described in humans interacting with 19 chemokine receptors reflecting the redundancy of the system (Chow et al., 2014).

1.3.1 The role of chemokines in tumors

Tumor cells, as well as their microenvironment constitutively produce a variety of chemokines. In the context of cancer, chemokines are discussed to have controversial anti-tumor but also tumor-promoting properties including enhanced tumor growth, invasion and metastasis and stimulation of angiogenesis. Furthermore, as key players of cell migration, chemokines are frequently involved in the recruitment of several cell types into the tumor milieu (Raman et al., 2007; Müller et al., 2001; Keeley et al., 2011; Hojo et al., 2007). For instance, CXCL8, CXCL12 and CCL5 are well-characterized chemokines promoting the growth of malignant cells by enhancing their proliferation and survival (Zhu et al., 2004; Smith et al., 2004; Singh et al., 2018). In breast and prostate cancer, the recruitment of immunosuppressive tumor-associated macrophages (TAMs) is linked to the tumoral expression of the chemokine CCL2, thus associated with a pro-tumoral function (Soria et al., 2011; Zhang et al., 2010). In addition, cancer-associated fibroblasts are capable to produce chemokines, which leads to the recruitment of immunosuppressive Treg cells, inducing tumor progression and development of metastasis (Liao et al., 2009).

On the other hand, numerous studies observed a positive correlation of tumoral chemokine expression and attraction of effector T cells with anti-tumor abilities. In this context, an increased expression of CXCL9 and CXCL10 by tumor tissue is correlated with enhanced tumor-infiltration of CD4⁺ and CD8⁺ lymphocytes that express high levels of the cognate receptor CXCR3. Here, chemokines play an important role in directing TILs in tumors resulting in an anti-tumor effect (Gorbachev et al., 2007; Yang et al., 2006;). The importance of these chemokines is also seen in human tumor biopsies. For instance, colorectal carcinomas with high CXCL10 levels showed an abundance of TILs expressing CXCR3 (Musha et al., 2005). Another example for chemokine-mediated TIL recruitment to the tumor site is CX3CL1. This chemokine is produced by neuroblastoma or colorectal cancer cells and has the ability to attract and activate lymphocytes. Therefore, a high expression of CX3CL1 is associated with a better prognosis (Siddiqui et al., 2016; Ohta et al., 2005).

In summary, chemokines and their receptors represent a highly complex network and the functionality of chemokines in cancer is strongly depended on the circumstances in which

they are expressed as well as the stage of the disease. On the other hand, the expression of chemokine receptors by lymphocytes is a well-organized process depending on the differentiation and activation state of the cells and is influenced by the adjacent environment. Furthermore, naïve lymphocytes down-regulate receptors for homeostatic chemokines in favor of an up-regulation of inflammation-associated chemokine receptors during the development to effector cells (Mackay et al., 1990).

1.3.2 Arming tumor-specific T cells with chemokine receptors to improve ACT

Because of their disseminated expression in cancer and their versatile role in tumor formation and progression, chemokines became an interesting target in cancer therapy as well as potential agent for immunotherapy (Homey et al., 2002). Current approaches in the area of ACT focus on the idea to improve T cell homing through the insertion of otherwise absent or insufficiently expressed chemokine receptors into tumor-specific effector cells to increase their limited recruitment to the target site (Table 1). In this context, high expression levels of CCL2 in mesotheliomas have been described. But at the same time, it was demonstrated that activated human T cells engineered to express a mesothelin-specific CAR construct exhibit only minimal expression of the cognate receptor CCR2. Therefore, the chemokine receptor CCR2b was co-transduced along with the CAR construct into T cells and the therapeutic efficiency of the genetically engineered T cells was investigated. In this study, treating mice with established tumors revealed that the additional modification of CAR T cells with the chemokine receptor CCR2b led to a 12.5-fold increase in tumor infiltration in comparison to T cells expressing only the CAR construct without the chemokine receptor. That, in turn, led to a significant increase in the therapeutic effect (Moon et al., 2011).

Over the last years, a limited number of studies focused on the additional genetic modification of CAR T cells to co-express chemokine receptor(s) matching the tumors chemokine profile to enhance tumor-infiltration by CAR T cells (Table 1).

Table 1: Overview of studies examining the combination of CAR or TCR engineering with chemokine receptor expression to ameliorate the efficiency of cancer treatment.

CAR or TCR construct	Chemokine receptor	Malignancy	Reference
Anti-CD30 CAR	CCR4	Hodgkin lymphoma	Di Stasi et al., 2009
Anti-GD2 CAR	CCR2b	Neuroblastoma	Craddock et al., 2010
Anti-gp100 TCR	CXCR2	Melanoma	Peng et al., 2010
Anti-mesothelin CAR	CCR2b	Mesothelioma	Moon et al., 2011
Anti-EGFRvIII CAR*	CXCR4	Glioblastoma	Müller et al., 2015
Anti-OVA TCR	CCR2	Lymphoma	Garetto et al., 2016
Anti-OVA TCR	CCR4	Pancreatic cancer	Rapp et al., 2016

* NK cells engineered to express the chimeric antigen receptor

All of these approaches achieved enhanced trafficking and anti-tumor activity of TCR- or CAR-modified T cells when combined with the expression of a chemokine receptor.

It is conceivable that this strategy can be translated to other tumors with a specific and restricted chemokine expression pattern to improve tumor homing under the guidance of appropriate chemokine receptors. Since many different cancers are associated with an extensive chemokine network, it is of vital importance to identify suitable chemokine and chemokine receptor interaction patterns to optimize the tumor homing of adoptively transferred tumor-specific T cells and enhance therapeutic benefits in the treatment of solid tumors (Balkwill et al., 2012).

1.3.3 The CXCL16-CXCR6 axis

Among the complex chemokine network, CXCL16 and CXCR6 are a unique chemokine-chemokine receptor pair: CXCL16 belongs to the CXC chemokine family and exists both in a transmembrane and a soluble form (Wilbanks et al., 2001). The transmembrane protein is cleaved by metalloproteinases of the ADAM family, ADAM10 and ADAM17, yielding the soluble form (Schramme et al., 2008). CXCL16 interacts with its sole receptor CXCR6, also known as Bonzo. The activation of the pair is involved in several biological processes, including trafficking of lymphocyte subsets, cell adhesion, cell survival, muscle regeneration and brain development (Hattermann et al., 2008; Hara et al., 2006; Zhang et al., 2009).

Recent studies confirmed an over-expression of CXCL16 in distinct types of human cancer, such as lung (Hald et al., 2015), prostate (Darash-Yahana et al., 2009), renal (Gutwein et al., 2009), colorectal (Hojo et al., 2007), ovarian (Gooden et al., 2014), bladder (Lee et al., 2013), breast (Meijer et al., 2008) and pancreatic cancer (Wente et al., 1992). But the role of the CXCL16-CXCR6 axis in cancer is still unclear, since divergent functions have been reported

including increased tumor growth, invasion, metastasis and angiogenesis associated with a poor prognosis (Ke et al., 2017; Deng et al., 2010; Darash-Yahana et al., 2009; Gooden et al., 2014; Ha et al., 2011). In contrast, colorectal carcinoma and tumors high in CXCL16 expression revealed an increased number of CD4⁺ and CD8⁺ lymphocytes and a better outcome than weakly CXCL16 expressing tumors (Hojo et al., 2007). Furthermore, mice lacking CXCR6 exhibited a more restricted number of TILs resulting in tumor progression in a breast cancer model (Matsumura et al., 2008). Thus, CXCL16 expression might also serve as a positive prognostic marker as described in the context of renal cancer (Gutwein et al., 2009).

1.4 Research objectives

Up to now, the potential of TCR- or CAR-engineered T cells endowed with otherwise absent chemokine receptors has been verified in only a limited number of studies (Table 1). Therefore, the chemokine network represents an attractive research focus to further enhance the therapeutic benefits of ACT in solid tumors. For this approach, CXCL16 seems to be an interesting candidate. The chemokine is expressed in several solid tumor entities and a positive effect of CXCL16 on the homing of TIL in colorectal cancer has been outlined previously. Thus, it was proposed that the additional arming of TCR or CAR T cells with CXCR6 might improve ACT efficiency.

A previous doctoral student in the laboratory (Viktoria Blumenberg) showed a strong CXCL16 expression in murine pancreatic tumor cells resulting in higher chemokine levels in solid tumors than in any other healthy murine tissue. At the same time, she could demonstrate that the corresponding chemokine receptor, CXCR6, was absent in CD8⁺ lymphocytes. After genetic modification of ovalbumin (OVA)-specific OT-1 T cells with a CXCR6 expression vector, the chemokine receptor expressing T cells revealed an increased migration capability. Furthermore, her research indicated an enhanced T cell activation and target cell lysis upon co-culture with pancreatic tumor cells. Finally, a therapeutic effect of CXCR6-engineered OT-1 T cells in the treatment of established subcutaneous murine pancreatic tumors highlighted the potential of the CXCL16-CXCR6 interaction as a possible strategy to enhance ACT efficacy.

Based on these observations, the present thesis had the following objectives:

- to validate the previous findings with a second tumor model, which includes the investigation of the migration capability, T cells activation, *in vitro* and *in vivo* anti-tumor efficiency of CXCR6-expressing T cells

- to characterize the chemokine and chemokine receptor interaction and its ability to mediate cell adhesion
- to prove the suspected enhanced tumor homing of CXCR6-expressing tumor-specific T cells *in vivo*
- to validate the specificity of the therapeutic effect by using a CXCL16-deficient tumor model
- to characterize the trafficking activities of adoptively transferred CXCR6-expressing tumor-specific T cells *ex vivo*
- to examine the effects of CXCL16-secreting human tumor cells on CXCR6-expressing human T cells

2 Materials

2.1 Technical equipment

2-Photon microscope	Leica SP5IIMP	Leica Microsystems, Wetzlar, DE
Analytical balance	CPA1003S	Sartorius Laboratory, Göttingen, DE
Cell culture incubator	BBD 6220	Heraeus, Hanau, DE
Centrifuges	3L-R Multifuge	Heraeus, Hanau, DE
	Centrifuge 5318R	Eppendorf, Hamburg, DE
	Rotina 420R	Hettich GmbH, Tuttlingen, DE
Confocal microscope	Leica SP2 AOBS	Leica Microsystems, Wetzlar, DE
FACS	Canto II	BD Biosciences, Franklin Lakes, USA
	Fortessa	BD Biosciences, Franklin Lakes, USA
	Aria II	BD Biosciences, Franklin Lakes, USA
Heating block	Thermomixer 5436	Eppendorf, Hamburg, DE
iCELLigence RTCA	S16	ACEA Biosciences, San Diego, USA
Inverted microscope	Axiovert 40C	Zeiss Jena, DE
	Axiovert HAL 100	Zeiss Jena, DE
Laminar flow hood	HeraSAFE KS	Heraeus, Hanau, DE
LightCycler®	480 Instrument II	Roche Diagnostics, Rotkreuz, CH
MACS separator	QuadroMACS	Miltenyi Biotec, Bergisch Gladbach, DE
Multilabel plate reader	Mithras LB 940	Berthold, Bad Wildbad, DE
Photometer	NanoDrop 2000c	Thermo Fisher, Waltham, USA
pH-Meter	inoLab pH720	WTW GmbH, Weilheim, USA
Spinning disk confocal microscope	Nikon TiE	Nikon Instruments, Tokyo, JP
Thermocycler	T3	Biometra, Göttingen, DE
Vortex mixer	RS-VA10	Phoenix, Garbsen, DE
Water bath	Unitherm-HB	uni equip, München, DE

2.2 Materials

Cell culture flasks (T25 to T175)	Costar Corning, New York, USA
Cell culture plates (6- to 96-well)	BD Medical, Franklin Lakes, USA
ELISA microplates (96-well)	Costar Corning, New York, USA
Eppendorf tubes (0.5 ml, 1.5 ml, 2.0 ml)	Sarstedt, Nümbrecht, DE
FACS tubes	BD Biosciences, Franklin Lakes, USA
Nickel-coated 96-well plate	Thermo Fisher, Waltham, USA
Nylon filter SmartStrainer (100 µm, 30 µm)	Miltenyi Biotec, Bergisch Gladbach, DE
Pipetboy	Hirschmann Laborgeräte, Eberstadt, DE

Pipettes	Eppendorf, Hamburg, DE
Serological pipettes	Costar Corning, New York, USA
Syringes	BD Medical, Franklin Lakes, USA
Trans-well migration plates (8.0 µm)	Merck Millipore, Burlington USA

2.3 Chemicals and reagents

7-Aminoactinomycin D (7-AAD)	Sigma-Aldrich, St. Louis, USA
Albumin Fraction V (BSA)	Sigma-Aldrich, St. Louis, USA
Ammonium chloride	Sigma-Aldrich, St. Louis, USA
Biocoll Separation Solution (d = 1.077 g/ml)	Biochrom Merck Millipore, Darmstadt, DE
Calcein AM	BD Biosciences, Franklin Lake, USA
Calcium chloride	Sigma-Aldrich, St. Louis, USA
Collagenase D	Sigma-Aldrich, St. Louis, USA
Dimethyl sulfoxide (DMSO)	Sigma-Aldrich, St. Louis, USA
Disodium hydrogen phosphate dihydrate	Sigma-Aldrich, St. Louis, USA
DNase I	Roche, Mannheim, DE
Ethylenediaminetetraacetic acid (EDTA)	Sigma-Aldrich, St. Louis, USA
Ethanol 96-100 %	Sigma-Aldrich, St. Louis, USA
FACSFlow	BD Biosciences, Franklin Lake, USA
Fixable Viability Dye eFluor™ 780	eBioscience, San Diego, USA
Heparin sodium (25,000 I.U./5 ml)	Ratiopharm, Ulm, DE
HEPES	Sigma-Aldrich, St. Louis, USA
Isoflurane	CP Pharma, Burgdorf, DE
β-Mercaptoethanol	Sigma-Aldrich, St. Louis, USA
pegGOLD TriFast™	Peqlab, VWR International, Radnor, USA
Percoll Solution (d = 1.13 g/ml)	GE Health Care, Chicago, USA
Potassium chloride	Sigma-Aldrich, St. Louis, USA
Potassium hydrogen carbonate	Sigma-Aldrich, St. Louis, USA
RetroNectin®	TaKaRa, Kyoto,
Sodium chloride	Sigma-Aldrich, St. Louis, USA
Sulfuric acid (2 N)	Pharmacy of LMU, München, DE
Trypan blue	Sigma-Aldrich, St. Louis, USA
Trypsin (10 x)	PAA Laboratories, Pasching, AT
Tween-20	Roth, Karlsruhe, DE

2.4 Cytokines

HIS-tagged mouse CXCL16	SinoBiological, Wayne, USA
Recombinant human CXCL16	Peprotech, London, UK
Recombinant human IL-2	Peprotech, London, UK
Recombinant human IL-15	Peprotech, London, UK
Recombinant mouse CXCL16	Peprotech, London, UK
Recombinant mouse IFN- γ	Peprotech, London, UK

2.5 Antibodies

Table 2: Overview of all applied antibodies. Fluorochrome-conjugated antibodies were used for flow cytometry analysis and purified antibodies were utilized for lymphocyte stimulation in cell culture. Specified final concentrations have been used for FACS staining or activation of 10^6 cells

Specificity	Fluorochrome	Clone	Concentration	Manufacturer
Anti-human CD3	Purified	OKT3	2 μ g/ml	eBioScience
Anti-human CD8	Pacific Blue	SK1	1 μ g/ml	BioLegend
Anti-human CD28	Purified	CD28.2	2 μ g/ml	eBioScience
Anti-mouse CD3	Purified	145-2C11	1 μ g/ml	eBioScience
Anti-mouse CD3	PE	145-2C11	1 μ g/ml	BioLegend
Anti-mouse CD3	PE-Cy7	145-2C11	1 μ g/ml	BioLegend
Anti-mouse CD8	Pacific Blue	53-6.7	1.5 μ g/ml	BioLegend
Anti-mouse CD8	PerCP	53-6.7	1 μ g/ml	BioLegend
Anti-mouse CD11c	APC	N418	1 μ g/ml	BioLegend
Anti-mouse CD28	Purified	37.51	0.1 μ g/ml	eBioScience
Anti-mouse CD31	eFluor450	390	30 μ g/ml	eBioScience
Anti-mouse CD45.1	APC-Cy7	A20	1 μ g/ml	BioLegend
Anti-mouse CD90.1	Pacific Blue	OX-7	1.5 μ g/ml	BioLegend

2.6 Kits and assays

Bio-Plex Cell Lysis Kit	Bio-Rad, San Diego, USA
CD3 microbeads, human	Miltenyi Biotec, Bergisch Gladbach, DE
CountBright™ Absolute Counting Beads	Invitrogen, Carlsbad, USA
DuoSet® ELISA Human CXCL16	R&D Systems, Minneapolis, USA
DuoSet® ELISA Mouse CXCL16	R&D Systems, Minneapolis, USA
Dynabeads Human T-Activator CD3/CD28	Thermo Fisher, Carlsbad, USA
Dynabeads Mouse T-Activator CD3/CD28	Thermo Fisher, Carlsbad, USA
DC™ Protein Assay	Bio-Rad, San Diego, USA
Mouse IFN- γ ELISA Set	BD Biosciences, Franklin Lake, USA

SuperScript II Reverse Transcriptase kit Thermo Fisher, Carlsbad, USA

2.7 Cell lines, supplements and media

2.7.1 Cell lines

Table 3: Overview of cell lines used. All cell lines were tested to be mycoplasma free and human cell lines were identified by STR profiling.

Cell line	Species	Description	Medium	Reference
293Vec Eco	Human	Embryonic kidney	DMEM ^{****}	BioVec Pharma, USA
293Vec Galv	Human	Embryonic kidney	DMEM ⁺⁺⁺	BioVec Pharma, USA
293Vec RD114	Human	Embryonic kidney	DMEM ⁺⁺⁺	BioVec Pharma, USA
Capan-1	Human	Pancreatic cancer	DMEM ⁺⁺⁺	ATCC: HTB-79
E.G7-OVA	Murine	Lymphoma	mTCM	ATCC: CRL-2113
Flp-In TM 293	Human	Embryonic kidney	DMEM ⁺⁺⁺	Thermo Fisher, USA
MIA PaCa-2	Human	Pancreatic cancer	DMEM ⁺⁺⁺	ATCC: CRL-1420
PANC-1	Human	Pancreatic cancer	DMEM ⁺⁺⁺	ATCC: CRL-1469
Panc02-OVA	Murine	Pancreatic cancer	DMEM ⁺⁺⁺	Jacobs et al., 2011
PA-TU-8988T	Human	Pancreatic cancer	DMEM ⁺⁺⁺	DSMZ: ACC 162
Platinum-E	Human	Embryonic kidney	Plat-E medium	Morita et al., 2000
SUIT-2	Human	Pancreatic cancer	DMEM ⁺⁺⁺	Iwamura et al., 1987

⁺⁺⁺ supplemented with 50 ml FBS, 1 IU/ml penicillin, 2 mM L-glutamine

^{****} supplemented with 50 ml FBS, 1 IU/ml penicillin, 2 mM L-glutamine

The generation of stable retrovirus-producing cell lines for murine and human cell transduction has already been described by Ghani et al., 2007. In brief, pMP71 vectors carrying the appropriate sequence were stably introduced in the packaging cell lines 293Vec Eco or 293Vec RD114. Single cell clones were generated and indirectly screened for the highest level of virus production by determining transduction efficiency of primary T cells. This method was used to generate the virus producing cell lines 293Vec Eco-GFP, 293Vec Eco-mCherry, 293Vec Eco-CXCR6-2A-GFP, 293Vec RD114-GFP, and 293Vec RD114-CXCR6-2A-GFP.

Starting with Panc02-OVA or E.G7-OVA the CXCL16-overexpressing cell lines Panc02-OVA-CXCL16 or E.G7-OVA-CXCL16 were generated by transduction with pMXs vector containing the full-length murine CXCL16 cDNA (UNIPROT entry Q8BSU2). Flp-InTM 293-hCXCL16 cells were created by transduction of Flp-InTM 293 with pMXs vector containing the full-length human CXCL16 cDNA (UNIPROT entry Q9H2A7).

2.7.2 Supplements

Blasticidin (10 mg/ml)	InvivoGen, San Diego, USA
Dulbecco's modified Eagle's medium (DMEM)	PAA Laboratories, Pasching, AT
Fetal bovine serum (FBS, heat inactivated)	Gibco, Carlsbad, USA
HEPES (1 M)	Sigma-Aldrich, St. Louis, USA
Human serum	Sigma-Aldrich, St. Louis, USA
L-Glutamine (200 mM)	PAA Laboratories, Pasching, AT
Non-essential amino acids (NEAA)	PAA Laboratories, Pasching, AT
Penicillin/Streptomycin (100x)	PAA Laboratories, Pasching, AT
Puromycin (10 mg/ml)	InvivoGen, San Diego, USA
Roswell Park Memory Institute (RPMI) 1640	PAA Laboratories, Pasching, AT
Sodium pyruvate (100 mM)	PAA Laboratories, Pasching, AT
VLE-RPMI 1640	Biochrom, Berlin, DE

2.7.3 Media

Complete DMEM medium (DMEM⁺⁺⁺)

DMEM	500 ml
FBS	50 ml
Penicillin	1 IU/ml
Streptomycin	100 µg/ml
L-Glutamine	2 mM

Complete RPMI medium (RPMI⁺⁺⁺)

RPMI	500 ml
FBS	50 ml
Penicillin	1 UI/ml
Streptomycin	100 µg/ml
L-Glutamine	2 mM

Plat-E medium (DMEM⁺⁺⁺⁺)

DMEM	500 ml
FBS	50 ml
Penicillin	1 IU/ml
Streptomycin	100 µg/ml
L-Glutamine	2 mM
Blasticidin	10 µg/ml
Puromycin	1 µg/ml

293Vec Medium (DMEM⁺⁺⁺⁺)

DMEM	500 ml
FBS	50 ml
Penicillin	1 UI/ml
Streptomycin	100 µg/ml
L-Glutamine	4 mM

Murine T cell medium (mTCM)

RPMI	500 ml
FBS	50 ml
Penicillin	1 IU/ml
Streptomycin	100 µg/ml
L-Glutamine	2 mM
HEPES	1 mM
Sodium pyruvate	1 mM

Humane T cell medium (hTCM)

VLE-RPMI 1640	500 ml
Human Serum	12.5 ml
Penicillin	1 UI/ml
Streptomycin	100 µg/ml
L-Glutamine	2 mM
Sodium pyruvate	1 mM
NEAA (100 %)	1 %

Murine cytotoxicity medium

RPMI (w/o phenol red)	500 ml
FBS	5 ml
Penicillin	1 IU/ml
Streptomycin	100 µg/ml
L-Glutamine	2 mM
HEPES	1 mM
Sodium pyruvate	1 mM

Human cytotoxicity medium

RPMI (w/o phenol red)	500 ml
Human Serum	5 ml
Penicillin	1 UI/ml
Streptomycin	100 µg/ml
L-Glutamine	2 mM
Sodium pyruvate	1 mM
NEAA (100 %)	1 %

Digestion medium

RPMI	1 ml
Collagenase D	1 mg/ml
DNase I	0.05 mg/ml

Cryopreservation medium

FBS	900 µl
DMSO	100 µl

2.7.4 BuffersTransfection buffer (pH 6.76)

NaCl	1.6 g
KCl	74 mg
Na ₂ HPO ₄	50 mg
HEPES	1 g
Add 100 ml Aqua dest.	

Erythrocyte lysis buffer (pH 7.2)

NH ₄ Cl	8.92 g
KHCO ₃	29 mg
EDTA	1 g
Add 1 l Aqua dest.	

FACS buffer

PBS	500 ml
FBS	10 ml

2.8 Software

BD FACSDiva	BD Biosciences, Franklin Lake, USA
EndNote X7	Thomson Reuters, Calsbad, USA
Fiji software	Open Source Software
FlowJo 8.7	Tree Star, Ashland, USA
GraphPad Prism Version 5.0	GraphPad Software, La Jolla, USA
Leica LAS X 3.1 software	Leica Microsystems, Wetzlar, DE
Leica LCS software	Leica Microsystems, Wetzlar, DE
LightCycler® 480 software	Roche Diagnostics, Rotkreuz, CH
Microsoft Office 2016	Microsoft, Redmond, USA
SnapGene 4.2	GSL Biotech, Chicago, USA

3 Methods

3.1 Molecular biological methods

3.1.1 Generation of plasmids for retrovirus-mediated gene transfer

All constructs were generated by overlap extension PCR and recombinant expression cloning into the retroviral pMP71 or pMXs vector. To co-express mCXCR6 or hCXCR6 with GFP, the full-length of murine *Cxcr6* (UNIPROT entry Q9EQ16 amino acid 1-351) or human CXCR6 cDNA (UNIPROT entry O00574 amino acid 1-342) was linked to GFP by using a self-cleaving 2A peptide-encoding sequence (mCXCR6-2A-GFP or hCXCR6-2A-GFP). For fluorescence microscopy analysis, murine *Cxcr6*-encoding nucleotide sequence was fused to GFP with a non-cleavable linker (mCXCR6-GFP). For stable overexpression of the chemokine by tumor cells, the full length murine CXCL16 cDNA (UNIPROT entry A2CFE9) or human CXCL16 cDNA (UNIPROT entry Q9H2A7) was cloned into the pMXs vector.

3.1.2 RNA isolation and quantitative real-time PCR (qRT-PCR)

Total RNA was extracted from cells using pegGOLD TriFast™ according to the manufacturer's instructions. 2 µg of total RNA was used as a template for cDNA synthesis with the SuperScript II Reverse Transcriptase kit. Primers for qRT-PCR were designed with the Roche Universal Probe Library Assay Design Center using NCBI GenBank sequences. 5' Primer TGA ACT AGT GGA CTG CTT TGA GC and 3' Primer GCA AAT GTT TTT GGT GGT GA combined with probe #103 were used for the analysis of murine *Cxcl16*. The LightCycler 480® system was used to perform and evaluate qRT-PCR analysis. Relative gene expression levels are shown as the expression level of the gene of interest in relation to the expression level of hypoxanthine phosphoribosyltransferase (*Hprt*).

3.2 Cell biological methods

3.2.1 General cell culture conditions

All tumor cell lines were cultured in cell culture flasks in incubators at 37 °C, 5 % CO₂, and 95 % humidity and were handled under sterile conditions. Adherent cells were detached by incubating with trypsin solution for 5 to 10 min at 37 °C. Detached cells were spun down (400 x g, 5 min) and resuspended in the appropriate medium. Cells were supplemented with fresh medium three times a week or after reaching a confluence greater than 80 %. In order to determine cell numbers and viability, the cells were stained with trypan blue and manually counted using a Neubauer hemocytometer.

For the generation of Panc02-OVA tumor cells deficient for CXCL16, the CRISPR/Cas9 system was used as described previously (Ran et al., 2013). The U6-gRNA/CMV-Cas9-GFP

plasmid with a gRNA targeting exon 2 of the murine *Cxcl16* gene was purchased from Sigma-Aldrich, St. Louis, USA (gRNA sequence 5'-ACTTCCAGCGACACTGCCCTGG). Successful delivery of the plasmid into the tumor cells was confirmed by the expression of the GFP reporter gene and individual GFP-positive tumor cells were isolated by FACS sorting using BD FACS Aria II run on FACSDiva Software. An efficient gene knockout of single cell clones was validated by genome sequencing of the *CXCL16* gene and CXCL16 ELISA.

To expand CD8⁺ T cells, the cell suspension was transferred into tubes and centrifuged (5 min at 400 x g). Murine ovalbumin-specific OT-1 T cells were resuspended in mTCM and the cell concentration was adjusted to 10⁶ cells/ml, supplemented with 50 ng/ml human interleukin 15 (IL-15) and 50 μM β-mercaptoethanol. Human T cells were resuspended in hTCM and adjusted to 10⁶ cells/ml supplemented with 5 ng/ml IL-15, 0.2 μg/ml human interleukin 2 (IL-2) and 50 μM β-mercaptoethanol. T cells were cultured in 6-well plates or tissue culture flasks and maintained at 37°C, 5 % CO₂ and 95 % humidity. After two days of T cell culture, the cell number was quantified via trypan blue exclusion staining and the cells were re-cultured with 10⁶ cells/ml in respective media.

Capan-1 spheroids were generated by seeding 2,000 tumor cells in 100 μl DMEM⁺⁺⁺ into 96-well plates coated with 50 μl sterile 2 % agarose. Flp-InTM 293-hCXCL16 spheroids were grown as hanging drops in a humidity chamber (250 cells per 25 μl drop).

3.2.2 Generation of cell-free tumor supernatants

To generate cell-free supernatants, tumor cells were trypsinized, if necessary, spun down and counted. 2 x 10⁵ Panc02-OVA or 5 x 10⁵ E.G7-OVA cells per ml were seeded in 2 ml fresh medium with or without 20 ng/ml IFN-γ in 6-well plates and after 48 h the supernatants were harvested. For human tumor cells, 10⁶ cells per ml were plated in 2 ml fresh medium in 6-well plates and incubated for 72 h. Supernatants were centrifuged twice at 400 x g for 5 min in a conical Falcon tube to remove tumor cells. After that, supernatants were used for migration assays.

3.2.3 Isolation of primary murine T cells

OT-1, CD45.1 OT-1 or CD90.1 OT-1 mice were killed by cervical dislocation and the spleens were transferred into sterile tubes containing mTCM. Mashing the organ through a 100 μm and 30 μm cell strainer generated a single cell suspension. Cells were spun down (400 x g, 5 min) and red blood cells were depleted by using 3 ml erythrocyte lysis buffer. After 2 min, mTCM was added and the cells were centrifuged. After quantification, a sufficient number of

splenocytes was cultured for 48 h in mTCM supplemented with 4 µg/ml IL-2, 50 µM β-mercaptoethanol, 1 µg/ml anti-mouse CD3 and 0.1 µg/ml anti-mouse CD28 antibodies.

3.2.4 Isolation of primary human T cells

50 to 100 ml peripheral blood was drawn from irreversibly anonymized healthy donors using a 50 ml syringe covered with 20 IU heparin sodium per ml blood. For peripheral blood mononuclear cell (PBMC) isolation a density gradient with Biocoll (d = 1.077 g/ml) was used. First, the blood was diluted 1:1 with isotonic NaCl solution and 30 ml of the diluted blood was carefully layered over 15 ml Biocoll in a 50 ml Falcon tube. After a centrifugation step at 1,000 x g at 20 °C without a brake, the interphase ring containing PBMCs was aspirated and transferred to a new 50 ml Falcon tube. The cells were washed twice with isotonic NaCl solution (500 x g, 10 min, 20 °C) before separating of T cells using anti-human CD3 MicroBeads following the manufacturer`s protocol. 10⁶ cells/ml CD3⁺ human T cells were absorbed in hTCM supplemented with 5 ng/ml IL-15, 0.2 µg/ml IL-2, 50 µM β-mercaptoethanol and human T-Activator anti-CD3- anti-CD28 Dynabeads (33 µl per 10⁶ cells). Next, the T cells were cultured in 6-well plates, which have been coated with 2 µg/ml anti-human CD3 and 2 µg/ml anti-human CD28 antibodies the previous day. After two days of cell culture, the cells were used for transduction.

3.2.5 Retroviral transduction of murine T cells

The transduction of primary murine OT-1 T cells was conducted following a previously described protocol (Kobold et al., 2015). In brief, the ecotropic packaging cell line Platinum-E (Plat-E) was plated in 6-well plates and after 16 to 24 h, when the cells were 70 % confluent, they were transfected using calcium phosphate precipitation. The transfection mix per 6-well consisted of 2.5 M CaCl₂, 18 µg retroviral pMP71 plasmid DNA and 150 µl transfection buffer in a total volume of 300 µl. The transfection mix was added dropwise to the PlatE cells, which afterwards were incubated at 37 °C, 5 % CO₂, and 95 % humidity for 6 h. After incubation, medium containing the transfection mix was replaced by 3 ml DMEM⁺⁺⁺ and the cells were cultured at 37 °C, 5 % CO₂, and 95 % humidity for about 48 h. For the transduction, virus-containing medium of the confluent 6-well plate was collected and replaced by mTCM. Then the virus-producing PlatE cells were incubated for further 24 h. After this period, the virus-containing supernatant was again collected and used for a second transduction hit. When working with 293Vec-Eco virus producing cell lines, 1.2 x 10⁶ cells were seeded into a 6-well plate and virus-containing supernatant was harvested one and two days after plating. Virus-containing supernatants were passed through a 0.45 µm filter and used for retroviral transduction.

For the retroviral transduction of primary murine OT-1 T cells, a 24-well plate was coated with 6.25 µg/ml RetroNectin® (o/n at 4 °C) to optimize the co-localization of T cells and virus particles (Hananberg et al., 1996). The filtered retroviral supernatant was spun down onto the RetroNectin® coated 24-well plate (3,000 x g, 120 min, 4 °C). Next, the supernatant was discarded and 10⁶ activated OT-1 T cells per well were added to the virus-coated plate. 16 to 24 h after the first transduction a second transduction with new retroviral supernatant was performed. The transduction efficiency was analyzed using flow cytometry analysis. Transduced T cells were cultured in mTCM supplemented with IL-15 and β-mercaptoethanol as described in 3.2.1.

3.2.6 Retroviral transduction of human T cells

293Vec-RD114 virus-producing cell lines were used to generate supernatants for human cell transduction. 1.2 x 10⁶ cells were seeded into a 6-well plate and retrovirus-containing supernatant was harvested one and two days after plating. The retrovirus was coated onto 24-well culture plates coated with 6.25 µg/ml RetroNectin®. 10⁶ activated human T cells in hTCM supplemented with IL-2, IL-15 and β-mercaptoethanol were seeded onto virus-coated wells. The following day, a second transduction was performed using the same protocol. T cells were checked for their transduction efficiency using flow cytometry analysis, expanded in hTCM supplemented with IL-2, IL-15 and β-mercaptoethanol and as described in 3.2.1.

3.2.7 Isolation of cells from organs

Organs were removed from sacrificed mice and transferred to 24-well plates containing PBS. All following steps, when possible, were performed on ice. Tumors were homogenized with scalpels and incubated in digestion medium at 37 °C for 30 min on a shaking heating block (800 rpm). Single cell suspensions were generated by mashing spleens, lymph nodes or digested tumor tissue through a 100 µm and 30 µm cell strainer. For lymphocyte isolation, tumor cell suspensions were resuspended in 2 ml PBS and layered over a density gradient of 9 ml 44 % Percoll (upper phase) and 6 ml 67 % Percoll (lower phase). After a centrifugation step at 800 x g for 30 min at 4 °C without brake, the interphase ring containing lymphocytes was aspirated, transferred to a new Falcon tube and washed with PBS.

3.2.8 Generation of organ lysates

Organs were removed from sacrificed mice and shock frozen with liquid nitrogen. After shedding and homogenization using a mortar, the frozen tissue powder was lysed with the Bio-Plex cell lysis kit according to the manufacturer`s protocol. Protein concentrations were quantified using the Bradford method. Absorbance at 750 nm was detected with a microplate

reader (Berthold Mithras LB940 multilabel plate reader). Finally, protein concentrations were calculated using a standard curve.

3.2.9 Confocal microscopy assay

To monitor the intracellular trafficking of CXCR6 after interaction with its ligand CXCL16, 5×10^3 CXCR6-GFP transduced T cells were stimulated with 10 ng/ml recombinant CXCL16 (Peprotech, Hamburg, Germany). Receptor trafficking was monitored over a period of 1 h using a Leica SP5 AOBS confocal microscope run on the Leica LAS X 3.1 software. Membrane-associated CXCR6 expression was quantified by blinded counting of at least 75 representative cells per time point.

3.2.10 Cell adhesion assay

First, murine 10^7 T cells were washed with PBS, resuspended in 1 ml PBS and labelled with 5 μ M calcein AM following the manufacturer's protocol. After labelling, T cells were washed twice with FACS buffer and pre-incubated with or without 9 pmol recombinant mouse CXCL16 in 100 μ l PBS (30 min at 37 °C). Nickel-coated 96-well plates were coated with 100 μ l 9 pmol His-tagged CXCL16 or 9 pmol BSA (1 h at room temperature). Coated wells were washed twice with wash buffer (PBS + 0.05 % Tween20). 0.2×10^6 pre-stimulated T cells were transferred to the CXCL16 or BSA-coated nickel plate. After 25-min incubation and washing twice with cold PBS (4 °C), attached cells were lysed with RIPA buffer according to the manufacturer's recommendations. Cell lysates were spun down at 15,000 x g at 4 °C for 5 min and the fluorescence of the supernatants was analysed using a microplate reader (Berthold Mithras LB940 multilabel plate reader). The number of adherent cells is proportional to the fluorescent intensity at 495 nm.

3.2.11 Migration and spheroid invasion assay

Murine and human T cell migration was investigated using trans-well migration assays. 10^6 transduced T cells were placed into the upper chamber of a trans-well plate with an 8 μ m pore filter. The lower chamber contained 50 ng/ml human recombinant CXCL16 or cell-free tumor supernatant (prepared as described in 3.2.2). After 4 h incubation at 37°C the number of migrated cells in the lower chamber was quantified using flow cytometry analysis and CountBright™ Absolute Counting Beads.

On day 7 of 3D culture, Capan-1 or Flp-In™ 293-hCXCL16 spheroids were co-incubated with 15,000 T cells. After 18 h of co-incubation, non-invaded T cells were removed by washing with PBS prior to staining with 1 μ g/ml 7-AAD in 100 μ l PBS (o/n at room temperature, protected from light). Next, spheroids were carefully washed with PBS and fixed with 4 %

paraformaldehyde (2 h, 4 °C). Samples were imaged using a selective plane illumination microscope and invaded T cells were quantified using Fiji software as described previously (Rühland et al., 2015; Schmohl et al., 2015).

3.2.12 T cell stimulation and cytotoxicity assays

25,000 E.G7-OVA target cells were co-incubated with 0.25×10^6 T cells in a 96-well flat bottom plate for 18 h (effector to target ratio of 10:1). Following incubation, supernatants were collected, and T cell stimulation was determined using IFN- γ ELISA. In parallel, target cell lysis was quantified using the CytoTox 96® Non-Radioactive Cytotoxicity Assay according to the manufacturer`s protocol. Upon lysis, cells release lactate dehydrogenase (LDH) in the culture supernatant, which is measured with the colorimetric assay. Target cell lysis is calculated according to the following formula:

$$\frac{LDH^{of\ interest} - LDH^{of\ background} - LDH^{effector\ only}}{LDH^{total\ lysis} - LDH^{of\ background}} \times 100\ \%$$

3.3 Immunological methods

3.3.1 Enzyme-linked immunosorbent assay (ELISA)

Different human and murine ELISA kits were used to determine the cytokine concentration in cell supernatants, cell lysates and organ lysates. ELISA and buffer preparation were performed according to the manufacturer`s recommendations. Absorbance at 450 nm was measured with a microplate reader (Berthold Mithras LB940 multilabel plate reader). Protein concentrations were calculated using a standard curve, including background correction at 595 nm.

To determine the CXCL16 production in organs, all samples were diluted with reagent diluent (1 % BSA in PBS) to a protein concentration of 50 mg/ml. CXCL16 concentrations were calculated as pg cytokine per milligram protein in respective lysates.

3.3.2 Flow cytometry analysis (FACS)

To quantify the expression of defined surface molecules, cells were labeled with fluorophore-conjugated antibodies. First, single cell suspensions were washed by adding 100 to 1000 μ l FACS buffer followed by a centrifugation step (400 x g, 5 min, 4 °C). Cells were resuspended in FACS buffer, a defined concentration of antibodies and fixable viability dye for live/dead staining were added and incubated for 30 min at 4°C protected from light. In order to eliminate surplus antibodies, cells were washed with FACS buffer and resuspended in 100 μ l FACS buffer. To quantify specific cell populations, CountBright™ Absolute Counting Beads

were added prior FACS analysis according to the manufacturer's protocol. Cells were analyzed with FACS Canto II or FACS Fortessa both run on FACSDiva software. FACS data were analyzed using FlowJo 8.7.

For the separation of specific subpopulations, single cell suspensions were prepared and stained as described in 3.2.7. Cells of interest were sorted into a 1.5 ml tube containing FBS using BD FACS Aria II run on FACSDiva Software. FACS-sorted cells were cultivated (as described in 3.2.1) or lysed (as described in 3.1.2) for further studies.

3.4 Animal experiments

3.4.1 Care of laboratory animals

Five to eight weeks old female C57BL/6RJ wild-type mice were used for *in vivo* experiments. Mice were purchased from Janvier (Saint-Berthevin Cedex, France) or Charles River (Sulzfeld, Germany). C57BL/6RJ mice transgenic for an ovalbumin-specific T cell receptor (OT-1) were obtained from The Jackson Laboratory, US (stock number 003831). OT-1 mice were crossed with CD45.1 or CD90.1 congenic marker mice (obtained from The Jackson Laboratory, stock number 002014 or as a kind gift from R. Obst, Munich, Germany). Before the start of the experiments, all animals were held in the animal facility "Zentrale Versuchstierhaltung" for at least one week. Animal experiments have been approved by the local authority, Regierung von Oberbayern (reference number: 55.2.1.54-2532-90/12, 36-14 183-12 and 135-17).

3.4.2 Subcutaneous tumor models

Subcutaneous tumors were induced by injection of 2×10^6 Panc02-OVA or 5×10^5 E.G7-OVA-CXCL16 in 100 μ l PBS into the left flank of female mice. For treatment experiments, mice were injected intravenously with 10^7 T cells when tumors were palpable. Tumor size was measured three times a week using an electronic caliper and was defined as the area in mm^2 (length in mm x width in mm). Mice were sacrificed by achieving a tumor size $>250 \text{ mm}^2$ or tumor ulceration. For tracking experiments, mice were injected intravenously with 10^7 T cells, but here equal numbers of CXCR6- or control-transduced T cells were co-injected in one mouse. Four to five days after T cell transfer, mice were sacrificed, and organs were analyzed using flow cytometry analysis. To visualize tumor-infiltrating T cells, Panc02-OVA tumor-bearing mice were injected intravenously with T cells and the number of intratumoral T cells was quantified using two-photon laser scanning microscopy (TPLSM) five days after T cell transfer. To visualize intratumoral blood vessels, mice were injected intravenously with 3 μ g anti-mouse CD31 antibody (eFluor450) in 100 μ l PBS 30 min before sacrifice. Imaging of tumor-infiltrating T cells was performed using a resonant scanning Leica SP5IIMP system equipped with a Spectra Physics MaiTai DeepSee Ti:Sa pulsed laser tuned to 890 nm and a

20X NA 1.00 objective (Leica). Images with 15 to 20 μm spacing were acquired and processed using the Leica LAS X 3.1 software. The number of tumor-infiltrating T cells was quantified by counting at least six representative areas per tumor.

All studies are conducted randomized, blinded and with adequate controls. In accordance with the animal experiment approval, tumor growth and health status of mice were monitored every other day.

3.5 Statistical analysis

Statistical analyses were performed using GraphPad Prism software 7.0. Arithmetic mean and standard error of the mean were calculated. Statistical significance between experimental conditions was analyzed using two-sided Student's t-test for unpaired samples. Mann-Whitney U test was used to determine significance comparing data points of individual mice. For *in vivo* experiments, tumor growth curves were analyzed by two-way ANOVA with correction for multiple testing by the Bonferroni method. Log-rank (Mantel-Cox) test was performed for significance testing of survival curves.

4 Results

4.1 Expression of CXCL16 and its receptor CXCR6 in a murine model

4.1.1 *In vitro* expression of the chemokine CXCL16 in murine tumor models

In previous studies, our group has shown a prominent expression of CXCL16 in murine pancreatic tumor tissue, while organs displayed lower expression levels (unpublished data). Because of its chemotactic capacity, CXCL16 and its receptor CXCR6 are an attractive system to induce an enhanced trafficking of cytotoxic T cells towards solid tumors.

To study the therapeutic relevance of the CXCL16-CXCR6 axis for adoptive cell therapy, two tumor models were used: The murine lymphoma cell line E.G7-OVA and the murine pancreatic tumor cell line Panc02-OVA. Since both murine tumor models express ovalbumin, TCR transgenic OT-1 T cells specific for the model antigen were used to examine the role of CXCR6 in engineered CD8⁺ T cells.

First, the production of CXCL16 by these murine tumor cell lines was investigated using ELISA. In addition to the initial tumor cells, CXCL16-overexpressing or CXCL16-knockout cells were generated and their CXCL16 secretion was analyzed.

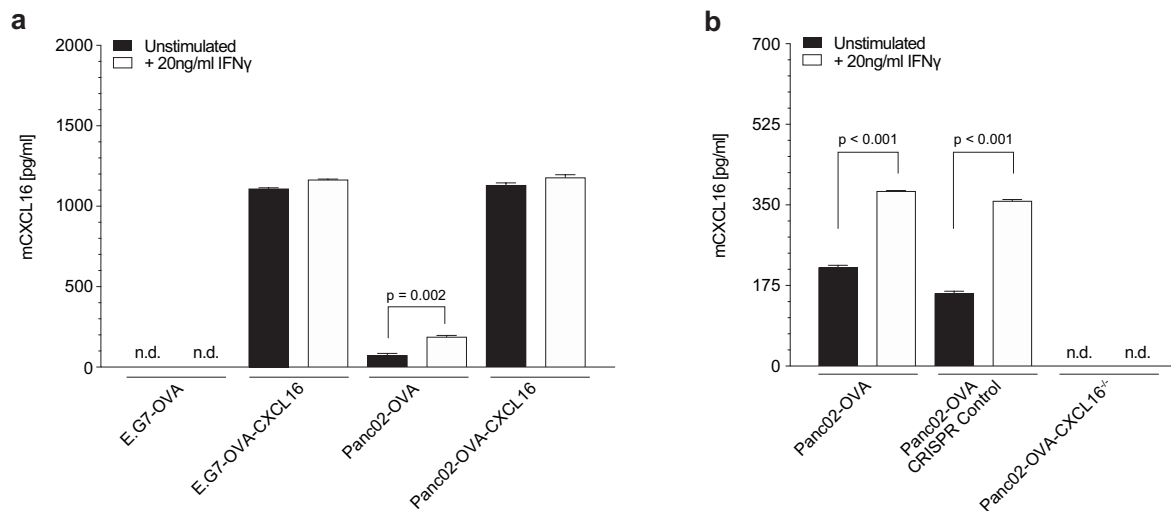


Figure 1: CXCL16 production by murine tumor cells.

a. The murine tumor cell lines E.G7-OVA, E.G7-OVA-CXCL16, Panc02OVA and Panc02-OVA-CXCL16 were stimulated with 20 ng/ml IFN- γ for 48 h and CXCL16 concentrations in supernatants were quantified by ELISA.

b. Wild-type Panc02-OVA, CRISPR Control and Panc02-OVA-*Cxcl16*^{-/-} tumor cells after stimulation with IFN- γ .

Representative values of three independent experiments are shown. Error bars represent SEM of duplicates (a) or triplicates (b). Statistical significance was calculated using two-sided Student's t-test. n.d., not detectable.

The murine lymphoma cell line E.G7-OVA showed no detectable CXCL16 expression, even after IFN- γ stimulation for 48 h. Stable transduction of the cell line with cDNA encoding the murine *Cxcl16* resulted in chemokine expression levels of about 1,100 pg/ml in the tumor

supernatants 48 h after seeding. The murine pancreatic tumor cell line Panc02-OVA expressed low levels of endogenous CXCL16. The concentration doubled by stimulation with IFN- γ for 48 h. After transduction with the murine *Cxcl16* cDNA, the pancreatic cell line expressed the chemokine in quantities comparable to E.G7-OVA-CXCL16 (Figure 1 a). To analyze CXCL16-mediated effects, a CXCL16-deficient knockout cell line was generated using the CRISPR/Cas9 system (Ran et al., 2013). As might be expected, the Panc02-OVA CRISPR Control cell line revealed CXCL16 concentrations similar to the wild-type Panc02-OVA cell line. For the Panc02-OVA-CXCL16 knockout cell line no secretion of the ligand was detectable, even after stimulation with IFN- γ for 48 h (Figure 1 b).

4.1.2 CXCL16 is expressed by tumor-infiltrating CD11c-positive myeloid cells

To further characterize the source of CXCL16, chemokine concentrations in Panc02-OVA-*Cxcl16*^{-/-} tumors were analyzed by ELISA. In addition, CD11c-positive myeloid cells were isolated from Panc02-OVA tumor tissue by FACS sorting and analyzed for *Cxcl16* mRNA expression using qPCR.

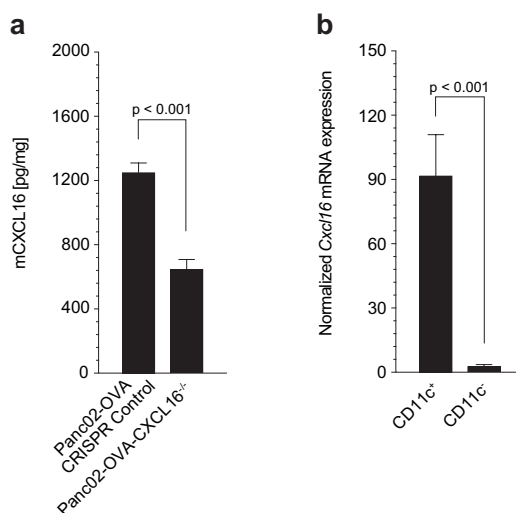


Figure 2: CXCL16 expression by Panc02-OVA-CXCL16^{-/-} tumors and tumor-infiltrating CD11c-positive myeloid cells.

a. Panc02-OVA-*Cxcl16*^{-/-} tumor cells were subcutaneously injected into the left flank of C57BL/6RJ mice. Once the predefined size had been achieved, tumors were harvested and intratumoral CXCL16 concentrations were determined using ELISA. Results are indicated as pg CXCL16 per mg total protein.

b. CD11c-negative and CD11c-positive cells were isolated from Panc02-OVA tumor tissue by FACS sorting and *Cxcl16* mRNA expression of the subpopulations was analyzed using qPCR. *Cxcl16* mRNA expression was normalized to *Hprt* mRNA expression.

Representative values of two (a) or three (b) independent experiments are shown. Error bars represent SEM with n = 10 (a) and n = 8 mice (b). Statistical significance was calculated by the Mann-Whitney U test.

Panc02-OVA-*Cxcl16*^{-/-} tumors showed a strongly decreased CXCL16 expression level compared to Panc02-OVA CRISPR Control tumors. Interestingly, the CXCL16 expression did not completely vanish but declined by 48 %, indicating the presence of additional CXCL16-expressing cells in the tumor microenvironment (Figure 2 a). The subsequent

analysis of tumor-infiltrating myeloid cells revealed a significantly lower *Cxcl16* mRNA expression in CD11c-negative cells compared to CD11c-positive cells (Figure 2 b). Consequently, CD11c-positive myeloid cells can be considered as an important intratumoral CXCL16 source in addition to the tumor cells themselves.

4.1.3 Genetic modification of murine cytotoxic T cells with CXCR6

According to literature, CXCR6 is almost absent from circulating CD8⁺ T cells with a fraction of less than 5 % CXCR6-positive cells under healthy conditions (Unutmaz et al., 2000). Therefore, cytotoxic antigen-specific OT-1 T cells were equipped with CXCR6 to force cell migration towards CXCL16 gradients produced by tumor tissue.

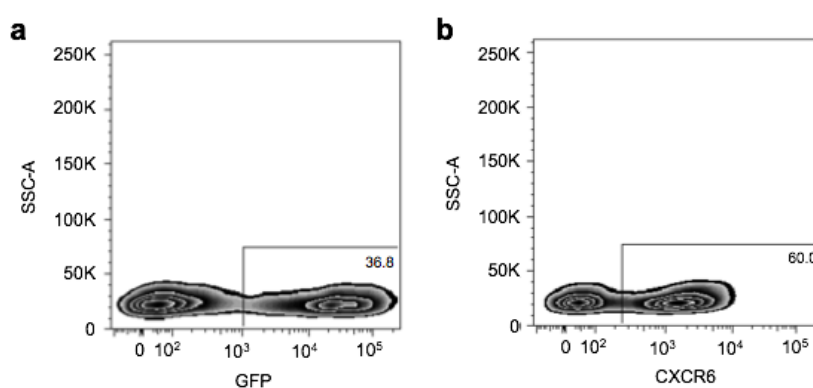


Figure 3: Representative retroviral transduction of murine CD8⁺ T cells.

a. Primary murine OVA-specific T cells (OT-1 T cells) were isolated from splenocytes and genetically modified using retroviral transduction to express the fluorescent protein GFP. Transduction efficiencies were examined using flow cytometry analysis.

b. Similarly, T cells were engineered to express the chemokine receptor CXCR6. Again, transduction efficiencies were examined using flow cytometry analysis.

First, the cDNA encoding murine CXCR6-2A-GFP (abbreviated to 'CXCR6⁺') was assembled in the retroviral expression vector pMP71 and used to transduce primary murine T cells. The efficiency of *Cxcr6* cDNA transfer into OT-1 T cells (hereinafter referred to as CXCR6-transduction) was quantified by flow cytometry analysis revealing a stable expression of CXCR6 by OT-1 T cells (Figure 3 b). GFP-modified T cells were used as a control to exclude secondary effects of the genetic modification (Figure 3 a). T cells with transduction efficiencies greater than 30 % were expanded for further *in vitro* or *in vivo* assays.

4.2 *In vitro* characterization of CXCR6-transduced T cells

4.2.1 CXCR6 mediates migration of primary murine T cells

The main objective of this research project was the development of a strategy for enhanced cytotoxic T cell migration and infiltration into solid tumors. Therefore, the functionality of the chemokine receptor expressed by T cells was investigated using trans-well migration assays.

Our group could previously show that CXCR6-expressing primary murine T cells specifically migrated towards recombinant CXCL16 in a dose-dependent manner (unpublished data). To demonstrate that this effect was also relevant for CXCL16 produced by tumor cells, trans-well migration assays with tumor cell-free supernatants were implemented.

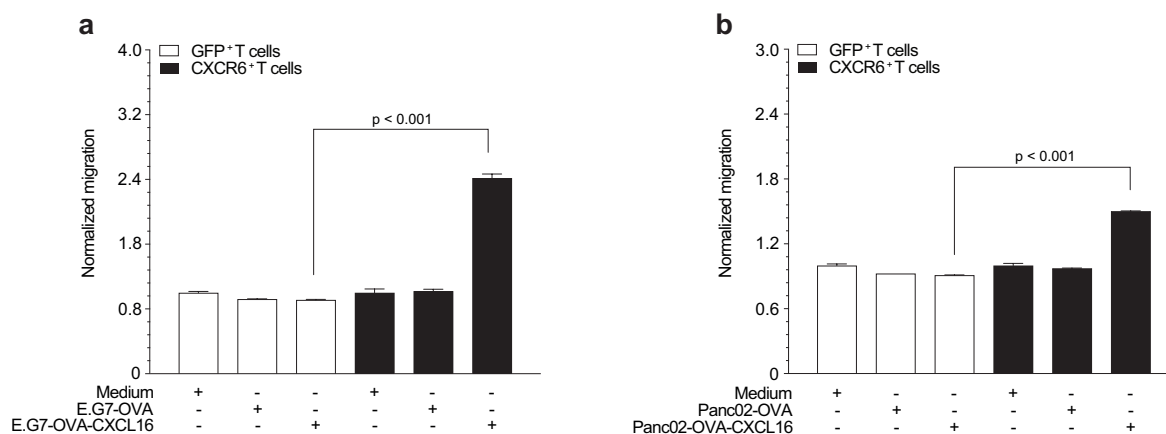


Figure 4: Migration of CXCR6-transduced T cells towards tumor cell supernatants.

a. OT-1 T cells were transduced with a retroviral vector encoding CXCR6 or GFP and migration capability towards E.G7-OVA supernatants was determined using trans-well migration assay.

b. Trans-well migration of CXCR6- or GFP-transduced OT-1 T cells towards Panc02-OVA supernatants. The number of CXCR6- or GFP-expressing migrated cells was quantified by flow cytometry analysis. Migration capacity was calculated as an increase of transduced T cells in the lower well compared to initial values (transduction efficiency) normalized to migration towards medium.

Representative values of three independent experiments are shown. Error bars represent SEM of triplicates and statistical significance was calculated using two-sided Student's t-test.

In a trans-well migration assay T cells engineered to express CXCR6 showed a significantly increased migration capability towards E.G7-OVA-CXCL16 (Figure 4 a) or Panc02-OVA-CXCL16 (Figure 4 b) supernatants compared to control GFP-transduced T cells. Migration was CXCL16 dependent, as only CXCR6-transduced T cells showed a definite enrichment while GFP-transduced T cells were not affected. T cell migration towards wild-type tumor cell supernatants, E.G7-OVA or Panc02-OVA, was absent due to the lack or moderate CXCL16 expression of the tumor cells. This observation emphasizes the importance of an appropriate CXCL16 gradient to efficiently stimulate T cell migration towards tumor tissue. Furthermore, this initial analysis of CXCR6-expressing T cells revealed that the transduced receptor was fully functional.

4.2.2 CXCR6 internalization and recycling upon CXCL16 engagement

The internalization and recycling of chemokine receptors in the presence of respective ligand has been described to play a crucial role in the sensitization or desensitization of receptor-expressing cell to the ligand (Neel et al., 2005). Therefore, the receptor trafficking upon CXCL16 binding in CXCR6-transduced T cells was studied.

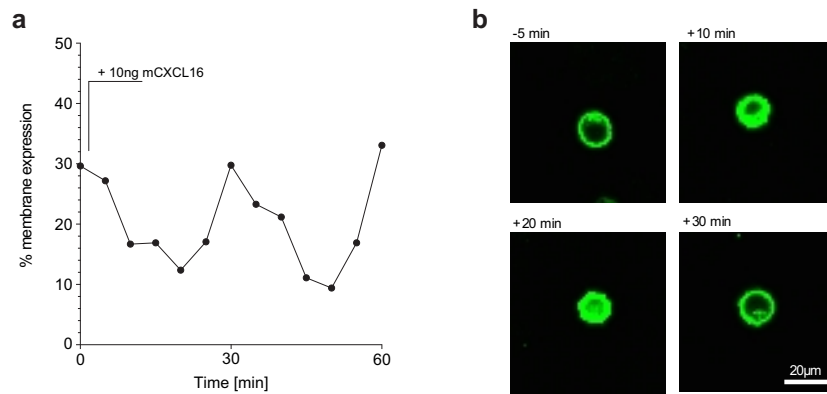


Figure 5: CXCR6 internalization and recycling.

a. 5,000 murine CXCR6-expressing T cells were stimulated with 10 ng/ml CXCL16 and receptor trafficking was monitored using confocal microscopy. Pictures were taken before adding CXCL16 and hereinafter every 5 min.

b. Microscopic images of T cells with representative receptor internalization status at indicated time points. Membrane-associated CXCR6 expression was quantified by blinded counting of at least 75 representative cells per time point. Representative values of three independent experiments are shown.

In the absence of ligand, the majority of the GFP-coupled CXCR6 was anchored in the membrane of the T cells. Upon ligand binding, the previously recorded membrane-associated fluorescence was changing towards an intracellular signal indicating rapid receptor internalization. The assimilated CXCR6 was recycled and re-expressed on the cell surface within 30 min (Figure 5). These findings suggest that the presence of CXCL16 did not permanently desensitize CXCR6-expressing T cells and the receptor maintained its functionality.

4.2.3 CXCR6 enhances recognition of CXCL16-producing tumor cells

Our group previously showed a time-dependent enhanced recognition of adherent tumor cells and T cell activation mediated by CXCR6 (unpublished data). The ameliorated tumor cell recognition led to an increased tumor cell lysis by CXCR6-transduced T cells compared to GFP-transduced T cells. To demonstrate that this effect was also transferable to another, non-adherent tumor cell line, E.G7-OVA cells were co-cultured with transduced OT-1 T cells and T cell activation and target cell lysis was investigated.

Results

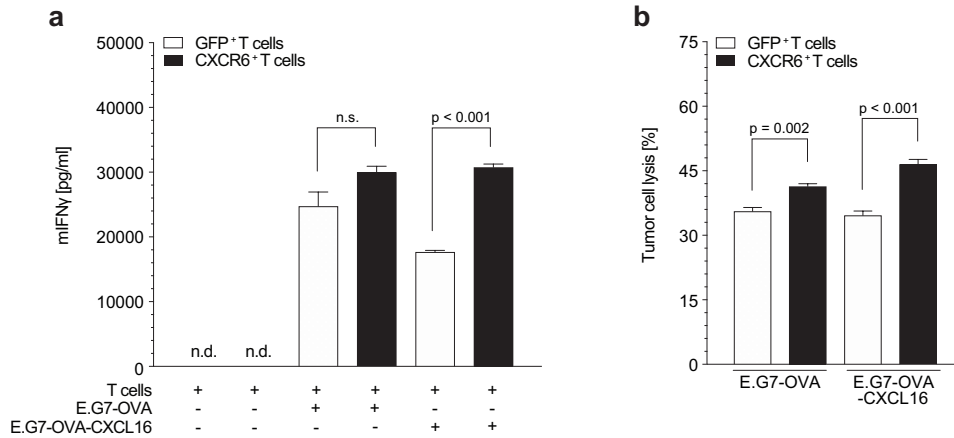


Figure 6: Tumor cell lysis and T cell activation upon co-culture of E.G7-OVA tumor cells with GFP- or CXCR6-transduced OT-1 T cells.

a. E.G7-OVA or E.G7-OVA-CXCL16 tumor cells were co-cultured in a 10:1 effector to target ratio with GFP- or CXCR6-transduced OT-1 T cells. After 18 h, T cell activation was examined by IFN- γ ELISA.

b. At the same time, tumor cell lysis was determined using the CytoTox 96® Non-Radioactive Cytotoxicity Assay.

Representative values of two (a) or three (b) independent experiments are shown. Error bars represent SEM of triplicates (a) or quadruplicates (b). Statistical significance was calculated using two-sided Student's t-test. n.d., not detectable.

Upon co-culture with E.G7-OVA tumor cells, no substantial difference in the activation level of GFP- and CXCR6-transduced T cells was identified. This was to be expected since E.G7-OVA tumor cells themselves do not produce CXCL16. The observed IFN- γ secretion for both GFP- and CXCR6-transduced OT-1 T cells is due to their OVA-specificity. However, CXCR6-transduced OT-1 T cells showed significantly increased IFN- γ levels compared to control-transduced OT-1 T cells after co-culture with E.G7-OVA-CXCL16. T cells cultured without tumor cells revealed no detectable IFN- γ secretion (Figure 6 a). As a consequence of an increased recognition of CXCL16-producing tumor cells, CXCR6-transduced OT-1 T cells demonstrated a noticeably higher E.G7-OVA-CXCL16 tumor cell lysis in comparison to GFP-transduced OT-1 T cells (Figure 6 b).

4.2.4 CXCR6 facilitates T cell adhesion to a CXCL16-positive surface

CXCL16 is a membrane-bound chemokine, which is released once cleaved by proteases (Schramme et al., 2008). While the soluble form mediates migration of CXCR6-expressing cells, the membrane-bound CXCL16 is associated with cell adhesion (Hara et al., 2006). In order to clarify whether CXCR6-transduced T cells are able to attach to CXCL16-positive surfaces, the adhesion ability to plate-bound CXCL16 was evaluated.

Results

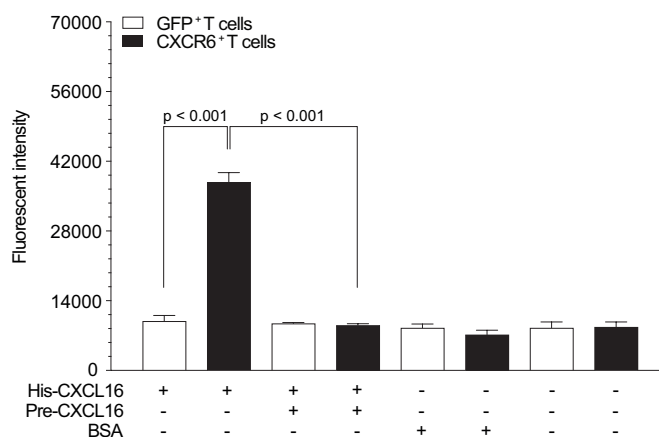


Figure 7: Analysis of the adhesion capability of murine CXCR6-transduced T cells.

GFP- or CXCR6-transduced T cells were stained with calcein and thereafter cultured on CXCL16-coated plates. After 30 min, the plates were washed, and the number of attached T cells was indirectly determined by the fluorescent signal. Pre-stimulation was conducted by 30 min incubation with soluble CXCL16 prior to culturing on CXCL16-coated plates.

Representative values of three independent experiments are shown. Error bars represent SEM of triplicates and statistical significance was calculated using two-sided Student's t-test.

CXCR6-transduced T cells exhibited a significantly enhanced adhesion capability to CXCL16-coated plates compared to GFP-transduced T cells (Figure 7). This effect was CXCL16-mediated, as CXCR6-transduced T cells did not adhere to control BSA-coated surfaces. Furthermore, pre-incubation with soluble recombinant CXCL16 abolished T cell adhesion to CXCL16-coated surfaces. This observation led to the assumption that the increased tumor cell lysis might be due to an enhanced adhesion of CXCR6-transduced T cells to CXCL16-producing tumor cells.

4.3 *In vivo* characterization of CXCR6-transduced OT-1 T cells

4.3.1 CXCR6 specifically improves the antitumor efficiency of adoptively transferred OT-1 T cells shown by delayed tumor growth *in vivo*

Based on the *in vitro* observations of an improved migration and tumor cell recognition by CXCR6-transduced OT-1 T cells, the relevance of the CXCL16-CXCR6 axis in connection with adoptive cell therapy was investigated. Therefore, the antitumor efficiency of CXCR6-transduced OT-1 T cells in comparison to control-transduced OT-1 T cells was determined in a subcutaneous tumor model.

Results

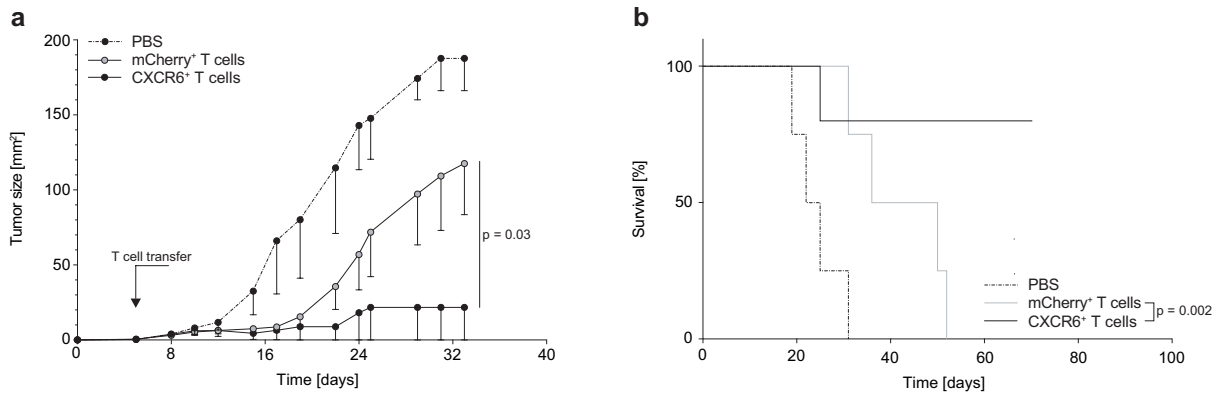


Figure 8: Treatment of E.G7-OVA-CXCL16-bearing mice with CXCR6-transduced OT-1 T cells.

a. 5×10^5 E.G7-OVA-CXCL16 cells were subcutaneously injected in the left flank of C57BL/6RJ mice. When the tumors were palpable, mice were randomized and treated with intravenous injection of 10^7 CXCR6- or mCherry-transduced OT-1 T cells. As a control, one cohort was injected with PBS. Tumor growth was measured three times a week.

Representative values of two independent experiments are shown. Error bars representing SEM of a minimum of four mice per group and statistical significance was calculated by two-way ANOVA with correction for multiple testing.

b. Kaplan-Meier survival curves of the same mice bearing subcutaneous E.G7-OVA-CXCL16 tumors treated as indicated. Mice were sacrificed based on the tumor size criteria.

Representative values of two independent experiments are shown. Log rank analysis comparing the survival curves were done with resulting p-values as indicated.

E.G7-OVA-CXCL16 tumor growth was significantly reduced in mice treated with CXCR6-transduced OT-1 T cells. As might be expected, control-transduced OT-1 T cells also showed a treatment effect due to their expression of an OVA-specific TCR (Figure 8 a). However, CXCR6-transduced OT-1 T cells mediated efficient tumor control with tumor rejection in four out of five mice over a period of 70 days resulting in prolonged survival of tumor-bearing mice in contrast to mice treated with mCherry-transduced OT-1 T cells (Figure 8 b).

Results

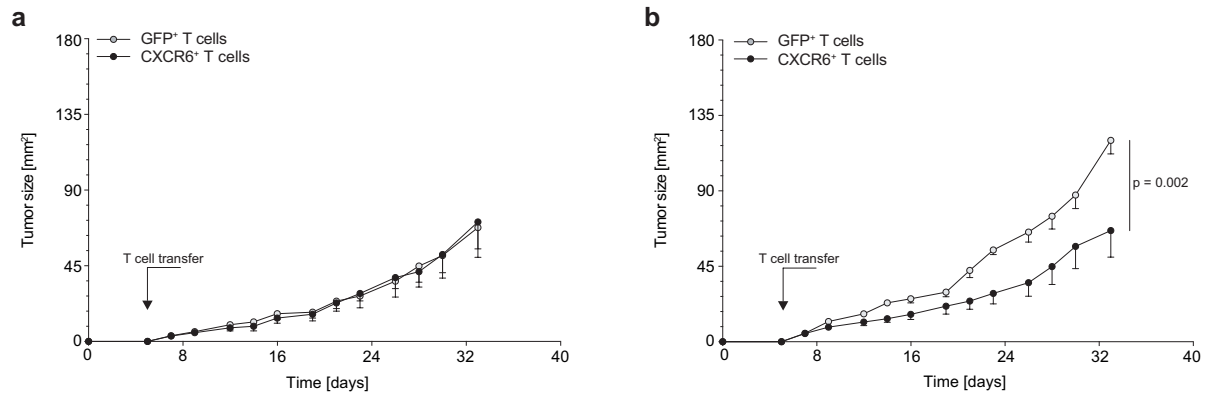


Figure 9: Treatment of Panc02-OVA-Cxcl16^{-/-} bearing mice with GFP- or CXCR6-transduced OT-1 T cells.

a. 2×10^6 Panc02-OVA-Cxcl16^{-/-} cells were subcutaneously inoculated in the left flank of C57BL/6RJ mice. When tumors were palpable, mice were randomized and treated with intravenous injection of 10^7 GFP- or CXCR6-transduced OT-1 T cells. Tumor growth was measured three times a week.

b. For comparison, 2×10^6 Panc02-OVA CRISPR Control tumor cells were subcutaneously inoculated, and mice were treated with 10^7 GFP- or CXCR6-transduced OT-1 T cells when tumors were palpable. Tumor growth was measured three times a week.

Representative values of three independent experiments are shown. Error bars representing SEM of a minimum of five mice per group and statistical significance was calculated by two-way ANOVA with correction for multiple testing.

Similarly, mice bearing Panc02-OVA-Cxcl16^{-/-} or Panc02-OVA CRISPR Control tumors were treated with GFP- or CXCR6-transduced OT-1 T cells. Comparable to the results in the E.G7-OVA-CXCL16 model, tumor growth in Panc02-OVA CRISPR Control tumor-bearing mice treated with CXCR6-transduced OT-1 T cells was retarded. By contrast, no difference in the tumor growth of Panc02-OVA-Cxcl16^{-/-} bearing mice after treatment with GFP- or CXCR6-transduced OT-1 T cells was observed (Figure 9). Overall, these results indicate an increased homing of CXCR6-transduced OT-1 T cells towards CXCL16-producing tumors. As described previously, tumor-infiltrating myeloid cells are able to produce CXCL16 resulting in a moderate CXCL16 expression in Panc02-OVA-Cxcl16^{-/-} tumors (Figure 2). In this context, the absent anti-tumor effect highlights the importance of a sufficient CXCL16 gradient to efficiently stimulate CXCR6-mediated T cell trafficking to the tumor site.

4.3.2 CXCR6 mediates T cell homing to tumor tissue

To further characterize the *in vivo* behavior of CXCR6-transduced OT-1 T cells, tracking experiments were performed in Panc02-OVA tumor-bearing mice. For this purpose, primary OT-1 T cells originating from congenic CD90.1-positive or CD45.1-positive OT-1 mice were used for transduction. In addition to the expression of GFP or CXCR6, transferred T cells were thus distinguishable from CD90.1-negative and CD45.1-negative recipient's T cells.

Results

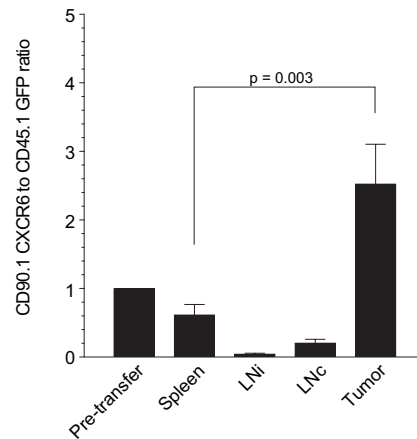


Figure 10: *In vivo* tracking of GFP- or CXCR6-transduced OT-1 T cells.

2×10^6 Panc02-OVA tumor cells were subcutaneously injected in the left flank of C57BL/6RJ mice. When tumors were palpable, mice were injected intravenously with a total of 10^7 CD90.1 CXCR6-transduced and CD45.1 GFP-transduced OT-1 T cells per mouse (CD90.1 CXCR6-transduced and CD45.1 GFP-transduced OT-1 T cells at a ratio of 1:1). Five days after treatment organs were harvested, single cell suspensions were generated and the number of transferred T cells in the indicated organs was quantified using flow cytometry analysis.

Representative values of three independent experiments are shown. Error bars represent SEM with $n = 10$ and statistical significance was calculated by the Mann-Whitney U test. LNi, ipsilateral lymph node; LNc, contralateral lymph node.

Before transfer in Panc02-OVA tumor-bearing mice, a mixture of CD90.1 CXCR6-transduced and CD45.1 GFP-transduced OT-1 T cells at a ratio of 1:1 was produced and verified by flow cytometry analysis. Tracking of the transferred T cells five days after injection revealed a specific accumulation of CD90.1 CXCR6-transduced OT-1 T cells compared to CD45.1 GFP-transduced OT-1 T cells in tumor tissue, but not in any of the other organs analyzed (Figure 10).

To confirm the findings of the flow cytometry analysis-based tracking experiment, the number of tumor-infiltrating CXCR6-transduced OT-1 T cells versus GFP-transduced OT-1 T cells in Panc02-OVA tumors was examined using *ex vivo* two-photon laser scanning microscopy.

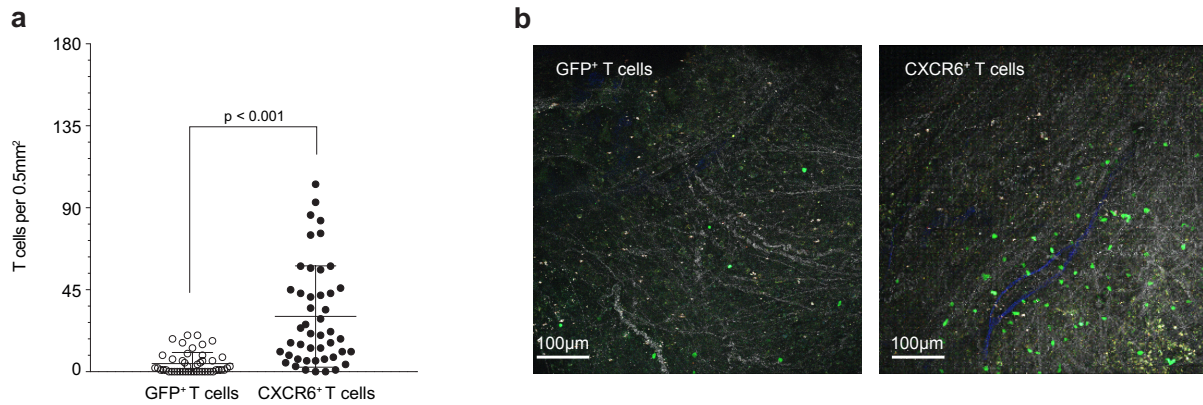


Figure 11: Quantification of tumor-infiltrating GFP- or CXCR6-transduced OT-1 T cells using two-photon laser scanning microscopy.

a. 2×10^6 Panc02-OVA tumor cells were subcutaneously inoculated in the left flank of C57BL/6RJ mice. When tumors were palpable, mice were injected intravenously with 10^7 GFP- or CXCR6-transduced OT-1 T cells per mouse ($n = 5$ mice per group). Five days after T cell transfer mice were injected with $3 \mu\text{g}$ anti-mouse CD31 antibody (eFluor450) 30 min before sacrifice to visualize intratumoral blood vessels. Images with 15 to $20 \mu\text{m}$ spacing of at least six representative areas per tumor were acquired using *ex vivo* two-photon laser scanning microscopy in collaboration with Dr. Remco T. A. Megens (IPEK, LMU Munich). Images were processed and the number of tumor-infiltrating T cells per 0.5 mm^2 tumor tissue was quantified

b. Microscopic images of representative tumor regions of mice treated with GFP- or CXCR6-transduced OT-1 T cells.

Representative values of two independent experiments are shown. Error bars represent SEM with $n = 5$ and statistical significance was calculated by the Mann-Whitney U test.

Ex vivo two-photon laser scanning microscopy from five distinct mice per group revealed an infiltration of both transferred OT-1 T cell populations in Panc02-OVA tumors. As suggested by the flow cytometry analysis-based tracking experiments, a significantly increased number of tumor-infiltrating CXCR6-transduced OT-1 T cells compared to GFP-transduced OT-1 T cells has been observed (Figure 11 a). The representative microscopic images show the quantitative differences in tumor-infiltration between GFP- and CXCR6-transduced OT-1 T cell, confirming their preferential tumor homing capability (Figure 11 b).

4.4 Expression of CXCL16 and its receptor CXCR6 in a human model

4.4.1 *In vitro* expression of the chemokine CXCL16 in human tumor models

The next step was to evaluate whether the observations seen in mice are applicable to human tumor models. First, the hCXCL16 production by several human pancreatic tumor cell lines was examined.

Results

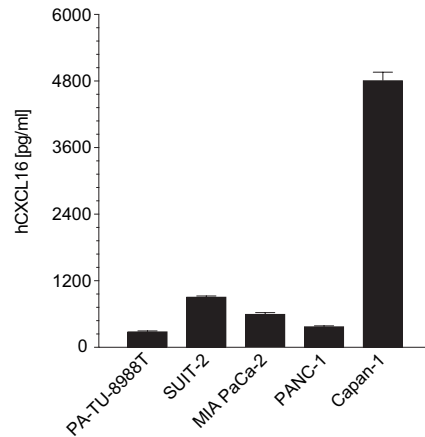


Figure 12: CXCL16 expression by human pancreatic tumor cell lines.

0.2×10^6 tumor cells were cultured for 72 h and hCXCL16 concentrations in tumor cell-free supernatants were quantified using ELISA.

Representative values of three independent experiments are shown. Error bars represent SEM of triplicates.

All human pancreatic tumor cell lines expressed and secreted hCXCL16 in varying concentrations; here PA-TU-8988T showed lowest hCXCL16 levels with 300 pg/ml and Capan-1 tumor cells revealed a strong chemokine secretion with about 4,800 pg/ml (Figure 12). This observation was an important prerequisite for the translation of the murine findings into the human setting.

4.4.2 Genetic modification of human cytotoxic T cells with a CXCR6-encoding retroviral vector

Similar to murine T cells, primary human CD3-positive T cells were equipped with human CXCR6 (hCXCR6) using retroviral transduction.

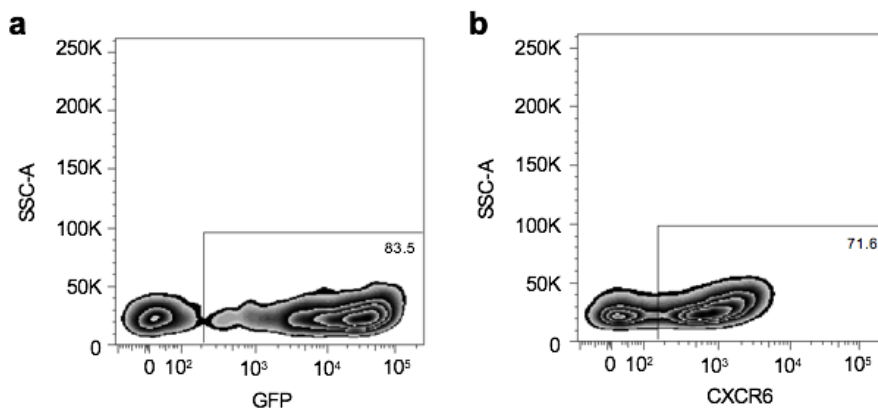


Figure 13: Representative retroviral transduction of primary human CD3-positive T cells.

a. Primary human T cells were isolated from PBMC and genetically modified using retroviral transduction to express the fluorescent protein GFP.

b. Expression of human CXCR6 by primary human T cells after retroviral transduction. Transduction efficiencies were examined using flow cytometry analysis.

The cDNA encoding human CXCR6-2A-GFP (abbreviated to 'hCXCR6') was assembled in the retroviral expression vector pMP71 and used for the transduction of primary human T cells. Flow cytometry analysis were conducted to validate the efficiency of human CXCR6 cDNA transfer (hereinafter referred to hCXCR6 transduction) revealing a stable expression of hCXCR6 in primary human T cells (Figure 13). As already described for the murine model, GFP-modified T cells were used as a control to exclude secondary effects of the retroviral transduction. Human T cells with transduction efficiencies greater than 30 % were expanded and used for following *in vitro* investigations.

4.4.3 hCXCR6 enables human T cells to migrate towards hCXCL16 gradients

The first step was to perform functional analysis to characterize the chemokine receptor-expressing human T cells. It was therefore analyzed whether hCXCR6-transduced T cells are able to recognize hCXCL16 and migrate towards chemokine gradients in trans-well migration assays.

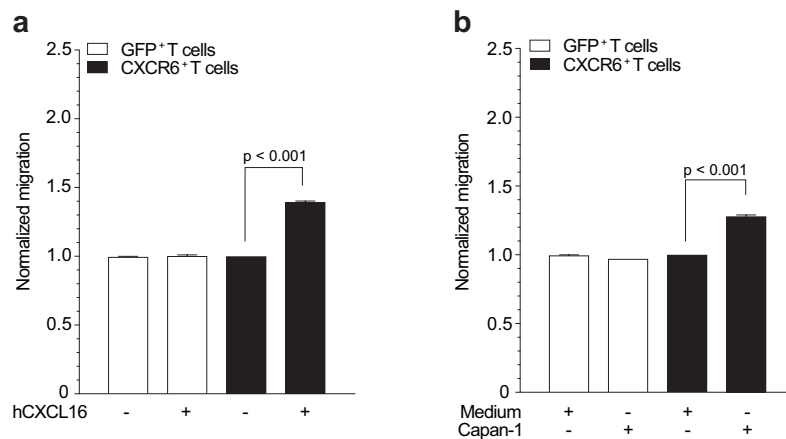


Figure 14: Migration of human CXCR6-transduced T cells towards recombinant CXCL16 and tumor cell supernatants.

a. Primary human T cells were either transduced with a retroviral vector encoding human CXCR6 or GFP and the migration capability towards 50 ng/ml recombinant human CXCL16 was confirmed using trans-well migration assays.

b. Trans-well migration assay of GFP- or hCXCR6-transduced primary human T cells towards cell-free supernatants of Capan-1 tumor cells. Migrated cells were quantified by flow cytometry analysis. Migration capacity was calculated as an increase of transduced T cells in the lower well compared to initial values (transduction efficiency) normalized to migration towards medium. Representative values of three independent experiments are shown. Error bars represent SEM of triplicates and statistical significance was calculated using two-sided Student's t-test.

When exposed to a CXCL16 gradient, hCXCR6- but not GFP-transduced human T cells migrated towards the recombinant protein (Figure 14 a). Since the recombinant protein did not affect GFP-transduced T cells, the observed migration of CXCR6-transduced T cells was receptor mediated. A comparable effect was observed when tumor cell-free supernatants of Capan-1 cells were used as migration stimulus. hCXCR6-transduced T cells were specifically attracted by the supernatant whereas GFP-transduced T cells exhibited no migration (Figure

14 b). This initial analysis of hCXCR6-transduced human T cells confirmed the expression of a fully functional chemokine receptor, which is able to recognize its ligand and mediates chemokine-dependent trafficking.

4.4.4 hCXCR6 mediates penetration of T cells into 3D tumor spheroids

Next, the invasion capability of hCXCR6-transduced T cells into tumor-like structures was studied using 3D spheroids. An important benefit of this *in vitro* 3D culture is the more physiological and spatial cell organization compared to common 2D culture providing a better representation of tumor tissue.

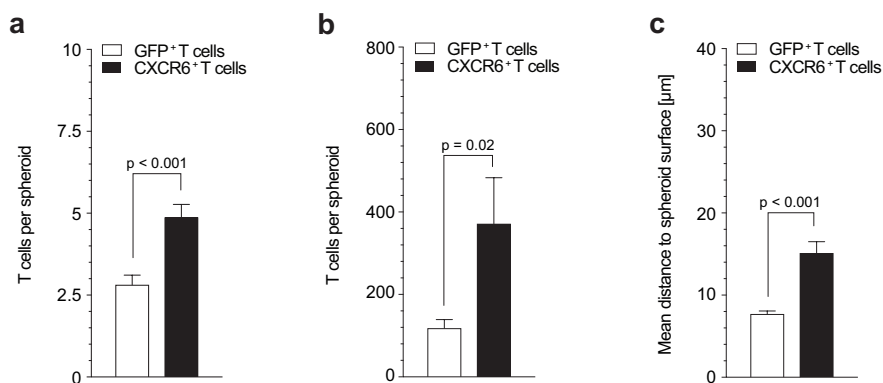


Figure 15: T cell invasion into 3D tumor spheroids.

a. Capan-1 tumor spheroids were co-cultured with GFP- or hCXCR6-transduced human T cells and the spheroid invasion capability was examined using spinning disc confocal microscopy.

b. Quantification of GFP- or hCXCR6-transduced human T cells penetrating Flp-In™ 293-hCXCL16 tumor spheroids.

c. Invasion depth of GFP- or hCXCR6-transduced human T cells penetrating Flp-In™ 293-hCXCL16 tumor spheroids measured as distance to the spheroid surface.

Values of three independent experiments are shown. Error bars represent SEM of at least 20 spheroids per group (a) or at least three spheroids per group (b, c). Statistical significance was calculated using two-sided Student's t-test.

For both Capan-1 and Flp-In™ 293-hCXCL16 tumor spheroids, a significantly increased number of invaded hCXCR6-transduced T cells in comparison to GFP-transduced T cells was determined. Differences in the number of invading T cells per spheroid between Capan-1 and Flp-In™ 293-hCXCL16 tumor spheroids are due to the smaller volume of Capan-1 tumor spheroids (Figure 15 a, b).

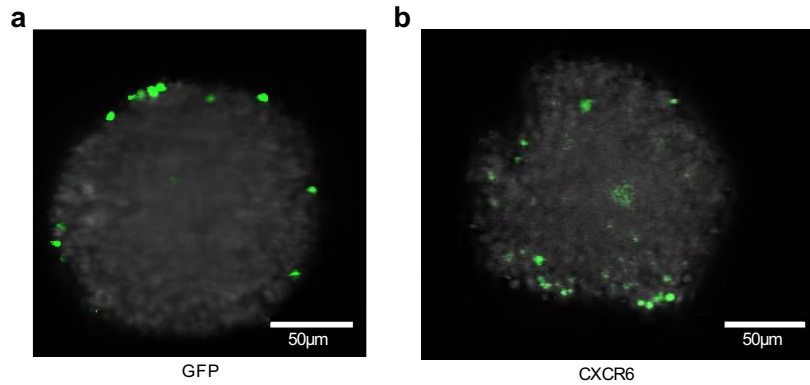


Figure 16: Visualization of spheroid invasion by human GFP- or hCXCR6-transduced T cells.

a. Flp-InTM 293-hCXCL16 3D spheroids were co-cultured with GFP-transduced human T cells and after 18 h T cell invasion into tumor spheroids was examined using spinning disc confocal microscopy.

b. Similarly, invasion of hCXCR6-transduced human T cells into Flp-InTM 293-hCXCL16 spheroids was determined.

Representative microscopic images of three independent experiments with at least three spheroids per group are shown.

In addition to quantitative differences, hCXCR6-transduced T cells achieved a greater invasion depth in Flp-InTM 293-hCXCL16 tumor spheroids compared to GFP-transduced human T cells (Figure 15 c, Figure 16). GFP-transduced human T cells mainly attached to the spheroid surface and were not able to invade the 3D structure (Figure 16 a). Conversely, hCXCR6-transduced T cells have the ability to invade the tumor-mimicking 3D cell formation, confirming their preferential homing capability into tumor-like structures (Figure 16 b).

Data shown in figure 2, 4-12 and 14-16 are part of a manuscript that is being prepared for publication.

5 Discussion

This study characterizes the impact of transgenic CXCR6 expression on the homing capacity of cytotoxic T cells into CXCL16-secreting tumor tissue. In the murine setting, CXCR6-transduced tumor-specific T cells showed increased migration abilities towards CXCL16-secreting tumor cells resulting in a tumor-specific homing of effector cells which was associated with an improved therapeutic effect. Furthermore, an enhanced adhesion of CXCR6-transduced T cells to CXCL16-positive surfaces was noticed, that could contribute positively to T cell-tumor cell interactions further improving the anti-tumor response. The observed migratory effect was transferable to the human model. Transgenic CXCR6 expression on primary human T cells enabled the recognition and effective migration towards human CXCL16 gradients. Furthermore, CXCR6-transduced human T cells were capable to penetrate 3D tumor structures. Thus, the CXCR6-CXCL16 interplay is a promising therapeutic approach to promote tumor homing of lymphocytes and thereby enhance anti-tumor immune responses.

5.1 IFN- γ amplifies the expression of CXCL16 by tumor cells

Previous data from our group have shown an up-regulated CXCL16 secretion by tumor cells upon stimulation with inflammatory cytokines, such as IFN- γ and TNF- α (unpublished data). In this study it could be confirmed that stimulation of tumor cells with IFN- γ leads to a 1.8 – 2.6-fold increase in CXCL16 secretion within 48 h. The effect could only be seen for tumor cells with endogenous CXCL16 expression, while the chemokine levels of CXCL16-overexpressing cells could not be further increased due to the lack of an IFN- γ sensitive promotor region in the retroviral vector used for the genetic modification of the tumor cells. Moreover, for validation, CXCL16-knockout tumor cells were not capable to produce CXCL16 with or without IFN- γ stimulation.

The expression of CXCL16 seems to correlate with inflammation (Lehrke et al., 2007). Not surprisingly, inflammation-associated cancers, such as ovary, breast, prostate, colon and liver cancer express high intratumoral levels of CXCL16 (Darash-Yahana et al., 2009). IFN- γ increases the level of *Cxcl16* mRNA but has no effect on ADAM10 and ADAM17 expression. Both metalloproteases are responsible for the cleavage of membrane-bound CXCL16 resulting in the soluble form (Abel et al., 2004). In context with CXCR6-transduced tumor-specific T cells, this observation is highly relevant since increased intratumoral CXCL16 levels will positively affect the recruitment of the genetically modified T cells. In this way, a stronger anti-tumor response can be expected resulting in an inflammatory microenvironment further increasing the intratumoral CXCL16 secretion and forming an amplification loop. Furthermore, an increased expression of membrane-bound CXCL16 might further enhance

T cell activation through greater adhesion and cell-cell interactions between tumor and effector cells.

Irradiation of tumor tissue induces an inflammatory state resulting in the secretion of cytokines, such as IFN- γ and TNF- α , into the TME (Lugade et al., 2008). This may be an explanation for the increased CXCL16 expression by tumor cells after ionizing radiation therapy (Matsumura et al., 2008). Therefore, the combination of local irradiation and adoptive transfer of CXCR6-expressing tumor-specific T cells provide a potential strategy to further enhance the anti-tumor effectiveness of the chosen model. Irradiation is a current standard treatment for cancer patients. Thus, a combination therapy is manageable to implement into the treatment regime. Furthermore, chemotherapy has been described to induce intratumoral expression of chemokines (Hong et al., 2011). Therefore, it will be of major interest to identify chemotherapeutic drugs enabling induction of intratumoral CXCL16 expression to enhance the attraction of CXCR6-engineered effector T cells into tumors and secondary metastasis.

5.2 CXCR6-mediated migration and adhesion improved target cell lysis by tumor-specific T cells *in vitro*

In this study, equipping T cells with the chemokine receptor CXCR6 resulted in a specific increase in cell migration towards CXCL16-positive tumor cell supernatants. Interestingly, this effect could only be observed with tumor cells overexpressing CXCL16. The moderate endogenous CXCL16 expression by wild-type Panc02-OVA tumor cells was not sufficient to stimulate migration of CXCR6-transduced T cells. This observation indicates a dose-dependent migration with a defined threshold value to initiate migration of CXCR6-expressing T cells. Moreover, this finding underlines the importance of a sufficient blood-tumor CXCL16 gradient as a requirement for an efficient *in vivo* tumor homing of CXCR6-transduced T cells. On the other hand, a simpler explanation might be that the artificial *in vitro* systems utilized do not mimic the *in vivo* situation.

As CXCL16 is associated with inflammation, the expression of the chemokine was reported for psoriatic skin lesions, a chronic inflammatory skin disease (Oh et al., 2009). Here, CXCR6-expressing CD8⁺ T cells isolated from psoriatic skin lesions showed a dose-dependent response to CXCL16 *in vitro* (Günther et al., 2012). Therefore, the findings of the presented study confirmed the already described dose-dependent chemotactic effect mediated by CXCR6.

Furthermore, a dose-dependent migration of lymphocytes transduced to express chemokine receptors has been reported previously. A study analyzing the trafficking of CXCR2-

transduced murine T cells indicated a dose-dependent migration of engineered T cells towards CXCL1 (Peng et al., 2010). The same was described for CX3CR1-transduced human T cells, which showed a dose-dependent migration towards CX3CL1 (Siddiqui et al., 2016). It should be emphasized that in the latter case, a concentration of 50 ng/ml recombinant CX3CL1 was not sufficient to trigger migration of transduced T cells. An efficient migration only occurred at a concentration of 100 ng/ml or more (Siddiqui et al., 2016). This dose-dependent migratory effect mediated by the expression of a chemokine receptor was confirmed in this study.

While the soluble form of CXCL16 is known to mediate migration of CXCR6-expressing cells (Matloubian et al., 2000), the membrane-bound form is associated with adhesion (Nakayama et al., 2003). In this study it could be shown that the transgenic expression of CXCR6 in cytotoxic T cells mediated both chemotaxis and adhesion to a CXCL16-covered surface. Therefore, the transduced receptor is able to fulfill all functions associated with the endogenous receptor expression.

As one of the first studies, Nakayama and colleagues described a CXCL16-induced chemotaxis of plasma cells via CXCR6 and also found an adhesive effect mediated by CXCL16 immobilized to plastic surfaces (Nakayama et al., 2003). The observations for both CXCR6-mediated characteristics are quite similar to the results presented for the transgenic receptor expression in cytotoxic T cells in the current study indicating a comparable receptor signaling.

Analyzing co-cultures of transduced OT-1 T cells and CXCL16-expressing tumor cells revealed an improved activation and a more efficient tumor cell lysis by CXCR6-transduced OT-1 T cells. This result can be explained by both the improved sensing and active movement of the T cells towards the CXCL16 gradient as well as the strengthened cell-cell contact mediated by CXCL16's adhesive capabilities, as described in this study. It is conceivable that the CXCR6-CXCL16-mediated adhesion will support the interaction of cytotoxic T cells and tumor cells resulting in an enhanced stimulation of the tumor-specific TCR through its antigen on the tumor cell. As a consequence, an increased effector activation will contribute to an improved anti-tumor response. Thus, CXCR6 has the potential to enhance tumor homing as well as subsequent effector function.

A study using ovalbumin-specific T cells in combination with the chemokine receptor CCR2 described no impact on the killing capacity nor on the activation of engineered T cells upon co-culture with E.G7-OVA tumor cells, but an improvement in T cell migration (Garetto et al.,

2016). The differences with the presented study might be due to the unique nature of CXCL16. While CCL2 only exists as soluble chemokine mediating chemotaxis, CXCL16 has the advantage of a dual function, migration and adhesion.

Several chemokines have been shown to provide co-stimulatory signals in T cells resulting in an increased T cell activation (Molon et al., 2005). This conclusion was made when T cells were stimulated by beads coated with anti-CD3 alone or with anti-CD3 plus CCR5 or CXCR4 agonists. The stimulation resulted in a T cell proliferation and activation comparable to that obtained by anti-CD28 co-stimulation (Molon et al., 2005). With the presented set of data it remains elusive whether CXCL16-binding to CXCR6-expressing CD8⁺ T cells represents a co-stimulatory signal resulting in a higher activation level. Therefore, prospective studies should be conducted to determine whether CXCL16 enhances T cell activation.

5.3 CXCR6 improves the anti-tumoral effects of ACT

In vivo functional analysis carried out in this study revealed a superior therapeutic effect mediated by CXCR6-transduced OT-1 T cells. In the lymphoma model E.G7-OVA-CXCL16, treatment with CXCR6-transduced OT-1 T cells resulted in retarded tumor growth with partial tumor clearance and prolonged overall survival in comparison to control mice. These observations suggested an improved CXCR6-mediated trafficking of adoptively transferred T cells and thereby enhanced anti-tumor activity. Along these lines, the potential of CXCR6 as mediator of lymphocyte recruitment was already described in inflamed tissue. For instance, CXCR6 regulates the recruitment of pro-inflammatory T cells into atherosclerotic lesions, although providing pro-atherogenic features in this context (Butcher et al., 2016).

In cancer, the significance of the CXCL16-CXCR6 axis in lymphocyte recruitment has been described by Matsumura and colleagues. In their study, mice lacking CXCR6 showed a reduced number of effector T cells in breast tumor tissue, which was associated with a limited anti-tumor response (Matsumura et al., 2008). Altogether, this indicates that CXCR6 is a promising candidate for the improvement of tumor homing in ACT.

However, it should not be neglected that in this study OT-1 T cells with almost 100 % tumor-specificity were transferred into tumor-bearing mice (data not shown). The percentage of tumor-specific CAR or TCR T cells among total transferred T cells in patients receiving ACT might be much lower. For instance, in a clinical trial investigating anti-EGFRvIII CAR-engineered T cells for the treatment of patients with malignant gliomas transduction efficiencies of approximately 50 % are described (NCT01454596). Preclinical studies in an animal model using anti-EGFRvIII CAR-engineered T cells with transduction efficiencies of

approximately 50 % showed impressive results in the treatment of glioma, but a result of the ongoing clinical trial is not yet available (Morgan et al., 2012). Thus, an improved recruitment of engineered tumor-specific T cells to the tumor tissue in clinical settings might be crucial for the success of ACT.

This conclusion is further supported by a recent study demonstrating an anti-tumor effect mediated by T cells without induced tumor specificity but engineered to express the chemokine receptor CX3CR1 (Siddiqui et al., 2016). This reveals the vital importance of an effective infiltration of effector T cells, even with unknown tumor specificity, into tumors and demonstrates the benefit of chemokine-mediated lymphocyte recruitment in ACT.

5.4 CXCR6-mediated therapeutic effects are dependent on a sufficient chemokine gradient

The therapeutic effect described for the lymphoma tumor model was absent when mice suffering from *Cxcl16*^{-/-} tumors were treated with CXCR6-transduced OT-1 T cells, whereas control CXCL16-producing tumors were associated with a treatment response. This finding demonstrates the dependency of the anti-tumor response on CXCL16-mediated T cell homing. Although tumor bystander cells were shown to express CXCL16, the reduced chemokine levels in *Cxcl16*^{-/-} tumors were not able to attract CXCR6-transduced OT-1 T cells. Therefore, no difference in the anti-tumor response between mice treated with CXCR6-transduced and control-transduced OT-1 T cells was observed. Furthermore, this observation underlines the existence of a dose dependent chemoattraction, probably with a certain threshold value of CXCL16 to ensure chemoattraction and extravasation of CXCR6-expressing T cells. This is in line with the lack of *in vitro* migration of CXCR6-transduced T cells towards moderate CXCL16 concentrations, as described above.

The importance of chemokines for the regulation of lymphocyte trafficking has been known since many years and chemokine-chemokine receptor interactions were shown to have a key role in lymphocyte development and immune responses in infected or diseased tissue (Stein et al., 2005). In the context of cancer, chemokine expression correlates with lymphocyte recruitment and improved clinical outcome due to the anti-tumoral immune response (Zhang et al., 2003). Moreover, a preclinical study analyzing the significance of the chemokine receptor CX3CR1 for the recruitment of T cells reported that a sufficient blood-tissue chemokine gradient is a crucial requirement for an effective tumor infiltration of T cells. The xenograft model of colorectal cancer used in this study indicated that shedding of the chemokine CX3CL1 by tumor cells led to an increased chemokine level in the blood and thereby eliminated the chemokine gradient essential for chemotaxis (Siddiqui et al., 2016).

Furthermore, similar observations were made in a murine model of melanoma. Here the chemokine ligands CCL5, CXCL9 and CXCL10 expressed by tumor cells were identified to recruit CD8⁺ T cells to tumor lesions. Lack of these chemokines was linked to a limited migration of cytotoxic T cells into the tumor and dampened the effectiveness of the antitumor immunity (Harlin et al., 2009). Overall, these findings are confirmed by the presented study, which indicated the crucial requirement of an established blood-tumor CXCL16 gradient for the therapeutic response mediated by adoptively transferred CXCR6-transduced T cells.

As mentioned above, tumors formed by *Cxcl16*^{-/-} tumor cells showed only a reduced chemokine expression but no complete absence of CXCL16. Subsequent analysis of tumor tissue indicated that CXCL16 is secreted by tumor-infiltrating CD11c-positive dendritic cells (DCs). Because of the immunostimulatory function of DCs and their ability to activate T cells, this was an interesting observation since CXCR6-mediated adhesion of cytotoxic T cells can strengthen their activation. In line with that, it was shown that CXCL16 enhances the interaction of DCs with cytotoxic T cells (Matloubian et al., 2000). The significance of the finding is reinforced by an enhanced expression of CXCL16 by DCs under inflammatory conditions (Tabata et al., 2005). Thus, an anti-tumor immune response might further stimulate DCs to express CXCL16 resulting in a greater chemokine gradient and chemotaxis of CXCR6-expressing T cells. Therefore, tumor-infiltrating CD11c-positive DCs contribute to development of a CXCL16 gradient and, moreover, stimulate the activation of CXCR6-expressing tumor-specific T cells, thus amplifying their anti-tumor effectiveness.

5.5 CXCR6 ameliorates T cell homing into tumor tissue

Flow cytometry analysis demonstrated a significantly enhanced trafficking of CXCR6-engineered OT-1 T cells into subcutaneous Panc02-OVA tumors in comparison to control transduced OT-1 T cells. Therefore, this finding confirmed the presumed improved tumor penetration by CXCR6-expressing tumor-specific T cells causing the enhanced anti-tumor activity.

Bobisse and colleagues described that the majority of adoptively transferred cells localize in healthy tissue, such as the spleen, while only a minority of T cells infiltrate the tumor tissue (Bobisse et al., 2009). The presented results rather identified the bulk of CXCR6-engineered T cells in tumor tissue and only a few cells were dispersed in healthy tissue indicating the tumor-specific trafficking. The efficient homing capacity of CXCR6-transduced T cells and the association with a therapeutic effect supports the hypothesis that a lacking tumor infiltration is a main limitation of ACT in solid tumors.

In the past, it was shown that tumors frequently progress even in the presence of a large number of circulating, tumor-specific T cells (Rosenberg et al., 2005). This is confirmed by clinical studies with limited response rates after immunization with cancer vaccines. Despite the successful generation of tumor-specific T cells, those cells failed to mediate effective immunologic tumor destruction (Rosenberg et al., 2004b). Even with ACT following lymphodepletion, only 50 % of metastatic melanoma patients showed an anti-tumor response, although up to 75 % of the circulating CD8⁺ T cells showed tumor specificity (Rosenberg et al., 2004a). The same effect was proven in this study. Although ovalbumin-specific effector T cells (control-transduced OT-1 T cells) were injected into E.G7-OVA tumor-bearing mice, only a limited anti-tumor response occurred, and all mice reached the pre-defined abort criteria due to the tumor burden. Only mice treated with tumor-specific T cells additionally expressing CXCR6 showed the ability of tumor clearance (four out of five mice). Therefore, the magnitude and durability of treatment response to ACT are closely associated with the number of tumor-infiltrating lymphocytes (Besser et al., 2010).

Based on the flow cytometry findings, a follow-up investigation using *ex vivo* two-photon laser scanning microscopy was performed to validate the enhanced tumor homing of CXCR6-transduced OT-1 T cells. This alternative method confirmed the more efficient homing of CXCR6-transduced OT-1 T cells in Panc02-OVA tumors.

Besides adhesion and chemotaxis, CXCL16 is associated with enhanced proliferation (Liang et al., 2018). Stimulation of lymphocytes with plate-bound CXCL16 was described to increase proliferation. This phenomenon was specifically mediated by CXCL16 since antibodies against the chemokine inhibited the proliferative effect (Darash-Yahana et al., 2009). It is interesting to consider this in context with CXCR6-expressing T cells in the tumor milieu. Flow cytometry and two-photon microscopy analysis demonstrated an accumulation of CXCR6-transduced T cell in the tumor tissue as a result of chemotaxis. Whether an increased proliferation of CXCR6-transduced T cells contributes to the intratumoral accumulation or whether this is exclusively a result of the enhanced tumor homing still remains to be elucidated.

Moreover, homing and trafficking of lymphocytes is mediated by a specific combination of adhesion molecules and chemokine receptors. Circulating lymphocytes roll along vessel walls, followed by adhesion to endothelial cells, crawling and extravasation (Herter et al., 2013). Different integrins have been described to be involved in this multistep process. For CD8⁺ T cells a VLA4-dependent rolling on vessel walls is described (Singbartl et al., 2001). Therefore, the $\alpha_4\beta_1$ integrin VLA-4 seems to be a crucial integrin mediating lymphocyte

transmigration (Nandi et al., 2004). Interestingly, CXCR6 signaling in murine and human lymphocytes was shown to activate VLA-4 leading to increased binding to VCAM-1 (Heydtmann et al., 2005). This observation suggests a role of CXCR6 in lymphocyte extravasation via VLA-4. Therefore, it would be interesting to investigate whether this signaling pathway is also involved in the trafficking of CXCR6-engineered T cell and still has to be examined.

5.6 CXCR6 enables human primary T cells to migrate towards CXCL16 gradients and invade tumor spheroids

As seen for the murine model, hCXCR6-transduced human T cells showed an improved migration capacity towards both recombinant CXCL16 and CXCL16-positive tumor cell supernatants. Thus, the effect size of the murine (1.5-fold increase in migration towards Panc02-OVA-CXCL16) and human migratory capability (1.3-fold increase in migration towards Capan-1) mediated by CXCR6 is reasonably comparable. A similar effect was described for the trans-well migration of CX3CR1-transduced human T cells towards recombinant human CX3CL1. Here, chemokine receptor-transduced T cells showed a 1.8-fold increased migratory capacity in comparison to control-transduced T cells (Siddiqui et al., 2016). Thus, the effect size is comparable with the one described in the present study.

Additionally, hCXCR6-transduced human T cells were able to infiltrate into 3D tumor cell spheroids and invaded deeper into the spheroids, while control-transduced T cells remained superficial. Together with the results of the trans-well migration assays, these results indicate that transgenic expression of the human chemokine receptor has equal properties as the murine chemokine receptor, such as improving chemotaxis and penetration of 3D structures. Whether the human chemokine receptor also mediates adhesion to CXCL16-positive surfaces still has to be proven.

After successfully equipping human T cells with improved tumor homing properties, the next critical step is to transfer a tumor antigen-specific CAR or TCR into the T cells mediating cytotoxicity. In this context, overexpression of the chemokine receptor CCR2b by anti-mesothelin CAR-expressing T cells already led to a 12.5-fold increase in tumor infiltration and significantly increased anti-tumor activity in a murine xenograft model (Moon et al., 2011). Therefore, the expression of CXCR6 should be combined with a CAR targeting tumor-specific antigens described for CXCL16-positive tumors. For instance, colorectal cancer is described to express high levels of CXCL16 (Hojo et al., 2007). On the other hand, there are preclinical and clinical studies (NCT03018405) investigating the potential of NKG2D-CAR T cell therapy for the treatment of colorectal cancer patients (Lonez et al., 2017). It would be

interesting to investigate whether the anti-tumor efficiency of those CAR T cells could be improved by the additional expression of CXCR6.

In general, the aim of future clinical trials should be to incorporate chemokine receptors into therapy protocols. In most cases ACT uses modified T cells, thus, minor protocol modifications are required including the transduction of chemokine receptors in addition to the TCR or CAR. This strategy has the potential to result in an incremental improvement of tumor homing of transferred T cells and an essential enhancement in the overall efficiency of ACT of solid tumors. Furthermore, the efficient tumor homing represents an important additional safety aspect because effector cells specifically accumulate on the target site instead of being distributed in the periphery where they can cause unpredictable side effects. The occurrence of severe adverse effects associated with adoptive T cell therapy, such as life-threatening cytokine storms, underline the importance to develop strategies improving tumor-targeted trafficking of transferred effector T cells (Fitzgerald et al., 2017).

For the future, the concept of chemokine receptor-transduced tumor-specific T cells could not only help to improve ACT of solid tumors but also represents a novel avenue to optimize personalized anti-cancer therapy. Based on tumor biopsies, patient specific chemokine expression profiles and tumor antigens can be identified enabling the genetic engineering of highly individualized T cell products with a tremendous therapeutic response.

5.7 Conclusion and perspective

In 2017 the FDA has approved the first two autologous CAR T cell therapies for the treatment of hematological malignancies. Since then, the interest in ACT as a treatment option of cancer has been growing. However, ACT efficiency still needs to be improved, especially for solid tumors. So far several strategies have been described to optimize the success of ACT focusing on enhanced T cell persistence, tumor recognition and activation of the innate immune system (Lim et al., 2017; Wang et al., 2014). Another critical step for ACT success in solid tumors and a prerequisite for TCR- or CAR-mediated antitumor effects represents an efficient tumor infiltration (Di Stasi et al., 2009). This study showed an improved trafficking of adoptively transferred CXCR6-expressing T cells into established CXCL16-secreting subcutaneous tumors, which was accompanied by an enhanced therapeutic effect. Therefore, ectopic expression of the chemokine receptor CXCR6 on transferred cytotoxic T cells is a promising approach to enhance antitumor activity. Most likely this strategy is complementary and synergistic with other approaches such as the transfer of tumor antigen recognizing TCR or CARs, which ultimately can lead to a significant improvement of ACT of solid tumors (Figure 17).

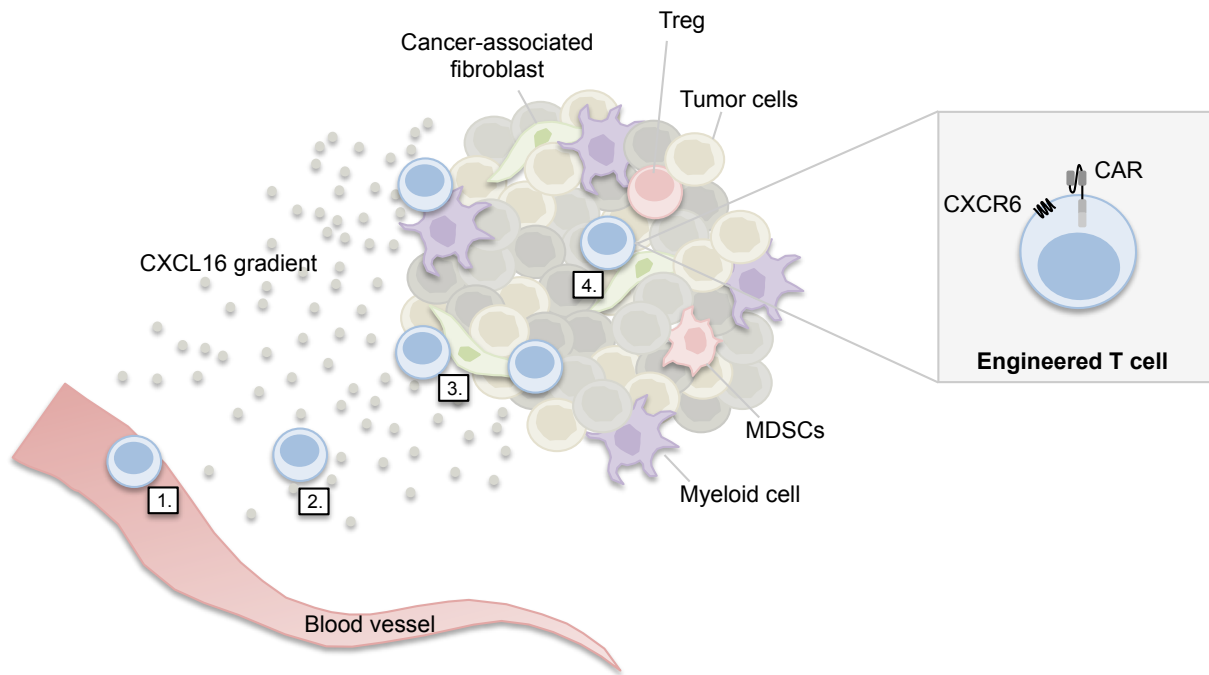


Figure 17: Schematic overview of the putative mode of action investigated in the present study. ACT using T cells engineered to express a tumor-specific CAR plus a chemokine receptor matching the tumors chemokine profile might improve the antitumor effect in solid tumors. The ectopic chemokine receptor promotes exit of the blood vessel (1), trafficking along the CXCL16 gradient produced by tumor cells and TME cells (2) and homing into the tumor tissue (3). Here the CAR mediates the cytotoxic function of the transferred T cell resulting in T cell activation and target cell lysis (4).

The ectopic expression of chemokine receptors on T cells mediating an improved recruitment to the tumor site is an approach, which is well compatible with current ACT protocols and has the potential for translation to the clinics. The vast majority of the ACT includes the transfer of T cells, which have been genetically engineered in order to enhance their antitumor specificity (Restifo et al., 2012). Thus, the addition of a chemokine receptor can be achieved with minor modifications of ACT protocols by two independent transductions or usage of a bicistronic vector expressing both transgenes.

This strategy of chemokine receptor modification could theoretically be translated to any tumor with previously identified chemokine profile. Especially patients with multiple metastases could benefit from such a treatment because a biopsy of a single accessible metastatic lesion could be used to identify the chemokine profile and therefore enables the selection of relevant chemokine receptor for the modification. However, so far only a limited number of studies focused on the combination of CAR- or TCR-engineered T cells and chemokine receptors to ameliorate tumor infiltration into solid tumors (Table 1). All of those preclinical approaches showed an increased tumor access of double-equipped T cells. An ongoing phase/II trial (NCT01740557) elucidating the potential role of chemokine receptors to improve the homing capacity of T cells started in 2015. Here the overexpression of CXCR2 and nerve growth factor receptor (NGFR) in TILs as a novel therapeutic option for

metastatic melanoma patients is investigated. Upon completion, this study will be of major significance for the application of chemokine receptors in this setting.

6 Summary

Adoptive T cell therapy using T cells engineered with tumor-specific CARs has been established as an effective treatment for hematological malignancies. In solid tumors, however, CAR T cell effectiveness remains anecdotal. While most current approaches aim to enhance T cell persistence or tumor recognition, the present study focuses on a strategy to enhance the effectiveness of ACT by improving T cell trafficking to the tumor tissue, which is a prerequisite of ACT of solid tumors. Therefore, the capability of the chemokine receptor CXCR6 to increase homing of cytotoxic T cells to tumor tissue expressing the corresponding chemokine CXCL16 was investigated. Of importance, this chemokine is expressed as a transmembrane molecule, mediating adhesion, as well as in a soluble form serving as chemoattractant. Furthermore, a broad variety of tumors produce CXCL16, whereas the majority of effector T cells lack the expression of CXCR6.

In the present study, the forced expression of CXCR6 resulted in an efficient migration of cytotoxic T cells towards CXCL16 gradients. Adhesive effects mediated by the transmembrane form of CXCL16 led to increased T cell activation and an enhanced target cell lysis. Based on these *in vitro* findings, the therapeutic activity of CXCR6-expressing tumor-specific T cells was investigated. In two different tumor models, treatment with CXCR6-expressing T cells retarded tumor growth, partially with tumor control, and prolonged survival. The therapeutic response correlated with enhanced trafficking and an increased number of tumor-infiltrating CXCR6-expressing T cells as shown by flow cytometry and two-photon microscopy. Tumor cells and non-tumor cells of the tumor microenvironment produce CXCL16. This promotes the recruitment of adoptively transferred T cells from blood vessels to the tumor tissue and reduces the chance of chemokine down-regulation during treatment. The chemoattractant effect of tumor-secreted CXCL16 on CXCR6-engineered T cells was transferable to the human system. Here, the next critical step will be the combination of a forced CXCR6 expression with a tumor antigen-specific CAR to equip human T cells with antitumor properties.

Together these data demonstrate that transgenic CXCR6 expression by tumor-specific T cells can overcome poor tumor homing of adoptively transferred T cells and therefore improves ACT response in murine solid tumor models.

7 Reference list

Abel S., Hundhausen C., Mentlein R., Schulte A., Berkhout T. A., Broadway N., Hartmann D., Sedlacek R., Dietrich S., Muetze B., Schuster B., Kallen K.-J., Saftig P., Rose-John S., Ludwig A. The transmembrane CXC-chemokine ligand 16 is induced by IFN- γ and TNF- α and shed by the activity of the disintegrin-like metalloproteinase ADAM10.

The Journal of Immunology 2004;172:6362-72.

Ahmed N., Brawley V. S., Hegde M., Robertson C., Ghazi A., Gerken C., Liu E., Dakhova O., Ashoori A., Corder A., Gray T., Wu M.-F., Liu H., Hicks J., Rainusso N., Dotti G., Mei Z., Grilley B., Gee A., Rooney C. M., Brenner M. K., Heslop H. E., Wels W. S., Wang L. L., Anderson P., Gottschalk S. Human epidermal growth factor receptor 2 (HER2) –specific chimeric antigen receptor–modified T cells for the immunotherapy of HER2-positive sarcoma.

Journal of Clinical Oncology 2015;33:1688-96.

Alexandrov L. B., Nik-Zainal S., Wedge D. C., Aparicio S. A. J. R., Behjati S., Biankin A. V., Bignell G. R., Bolli N., Borg A., Børresen-Dale A.-L., Boyault S., Burkhardt B., Butler A. P., Caldas C., Davies H. R., Desmedt C., Eils R., Eyfjörd J. E., Foekens J. A., Greaves M., Hosoda F., Hutter B., Illicic T., Imbeaud S., Imielinski M., Jäger N., Jones D. T. W., Jones D., Knappskog S., Kool M., Lakhani S. R., López-Otín C., Martin S., Munshi N. C., Nakamura H., Northcott P. A., Pajic M., Papaemmanuil E., Paradiso A., Pearson J. V., Puente X. S., Raine K., Ramakrishna M., Richardson A. L., Richter J., Rosenstiel P., Schlesner M., Schumacher T. N., Span P. N., Teague J. W., Totoki Y., Tutt A. N. J., Valdés-Mas R., van Buuren M. M., van 't Veer L., Vincent-Salomon A., Waddell N., Yates L. R., Australian Pancreatic Cancer Genome I., Consortium I. B. C., Consortium I. M.-S., PedBrain I., Zucman-Rossi J., Andrew Futreal P., McDermott U., Lichter P., Meyerson M., Grimmond S. M., Siebert R., Campo E., Shibata T., Pfister S. M., Campbell P. J., Stratton M. R. Signatures of mutational processes in human cancer.

Nature 2013;500:415-21.

Bajgain P., Tawinwung S., D'Elia L., Sukumaran S., Watanabe N., Hoyos V., Lulla P., Brenner M. K., Leen A. M., Vera J. F. CAR T cell therapy for breast cancer: Harnessing the tumor milieu to drive T cell activation.

Journal for Immunotherapy of Cancer 2018;6:34.

Balkwill F. R., Capasso M., Hagemann T. The tumor microenvironment at a glance.

Journal of Cell Science 2012;125:5591-96.

Besser M. J., Shapira-Frommer R., Treves A. J., Zippel D., Itzhaki O., Hershkovitz L., Levy D., Kubi A., Hovav E., Chermoshniuk N., Shalmon B., Hardan I., Catane R., Markel G., Apter S., Ben-Nun A., Kuchuk I., Shimoni A., Nagler A., Schachter J. Clinical responses in a phase II study using adoptive transfer of short-term cultured tumor infiltration lymphocytes in metastatic melanoma patients.

Clinical Cancer Research 2010;16:2646-55.

Bobisse S., Rondina M., Merlo A., Tisato V., Mandruzzato S., Amendola M., Naldini L., Willemsen R. A., Debets R., Zanovello P., Rosato A. Reprogramming T lymphocytes for melanoma adoptive immunotherapy by T-cell receptor gene transfer with lentiviral vectors.

Cancer Research 2009;69:9385-94.

Butcher M. J., Wu C.-I., Waseem T., Galkina E. V. CXCR6 regulates the recruitment of pro-inflammatory IL-17A-producing T cells into atherosclerotic aortas.

International Immunology 2016;28:255-61.

Chow M. T., Luster A. D. Chemokines in cancer.

Cancer Immunology Research 2014;2:1125-31.

- Craddock J. A., Lu A., Bear A., Pule M., Brenner M. K., Rooney C. M., Foster A. E. Enhanced tumor trafficking of GD2 chimeric antigen receptor T cells by expression of the chemokine receptor CCR2b. *Journal of Immunotherapy* 2010;33:780-8.
- Darash-Yahana M., Gillespie J. W., Hewitt S. M., Chen Y.-Y. K., Maeda S., Stein I., Singh S. P., Bedolla R. B., Peled A., Troyer D. A., Pikarsky E., Karin M., Farber J. M. The chemokine CXCL16 and its receptor, CXCR6, as markers and promoters of inflammation-associated cancers. *PLOS One* 2009;4:e6695.
- Deng L., Chen N., Li Y., Zheng H., Lei Q. CXCR6/CXCL16 functions as a regulator in metastasis and progression of cancer. *Biochimica et Biophysica Acta (BBA) - Reviews on Cancer* 2010;1806:42-9.
- Di Stasi A., De Angelis B., Rooney C. M., Zhang L., Mahendravada A., Foster A. E., Heslop H. E., Brenner M. K., Dotti G., Savoldo B. T lymphocytes coexpressing CCR4 and a chimeric antigen receptor targeting CD30 have improved homing and antitumor activity in a Hodgkin tumor model. *Blood* 2009;113:6392-402.
- Dudley M. E., Wunderlich J. R., Shelton T. E., Even J., Rosenberg S. A. Generation of tumor-infiltrating lymphocyte cultures for use in adoptive transfer therapy for melanoma patients. *Journal of Immunotherapy* 2003;26:332-42.
- Eggermont A. M. M., Chiarion-Sileni V., Grob J.-J., Dummer R., Wolchok J. D., Schmidt H., Hamid O., Robert C., Ascierto P. A., Richards J. M., Lebbé C., Ferraresi V., Smylie M., Weber J. S., Maio M., Bastholt L., Mortier L., Thomas L., Tahir S., Hauschild A., Hassel J. C., Hodi F. S., Taitt C., de Pril V., de Schaetzen G., Suciú S., Testori A. Prolonged survival in stage III melanoma with ipilimumab adjuvant therapy. *New England Journal of Medicine* 2016;375:1845-55.
- Fisher D. T., Chen Q., Appenheimer M. M., Skitzki J., Wang W.-C., Odunsi K., Evans S. S. Hurdles to lymphocyte trafficking in the tumor microenvironment: Implications for effective immunotherapy. *Immunological Investigations* 2006;35:251-77.
- Fitzgerald J. C., Weiss S. L., Maude S. L., Barrett D. M., Lacey S. F., Melenhorst J. J., Shaw P., Berg R. A., June C. H., Porter D. L., Frey N. V., Grupp S. A., Teachey D. T. Cytokine release syndrome after chimeric antigen receptor T cell therapy for acute lymphoblastic leukemia. *Critical Care Medicine* 2017;45:e124-e31.
- Ganesan A.-P., Johansson M., Ruffell B., Beltran A., Lau J., Jablons D. M., Coussens L. M. Tumor-infiltrating regulatory T cells inhibit endogenous cytotoxic T cell responses to lung adenocarcinoma. *Journal of Immunology* 2013;191:2009-17.
- Garetto S., Sardi C., Martini E., Roselli G., Morone D., Angioni R., Cianciotti B. C., Trovato A. E., Franchina D. G., Castino G. F., Vignali D., Erreni M., Marchesi F., Rumio C., Kallikourdis M. Tailored chemokine receptor modification improves homing of adoptive therapy T cells in a spontaneous tumor model. *Oncotarget* 2016;7:43010-26.

- Garrido F., Aptsiauri N., Doorduyn E. M., Garcia Lora A. M., van Hall T. The urgent need to recover MHC class I in cancers for effective immunotherapy.
Current Opinion in Immunology 2016;39:44-51.
- Geng Y., Shao Y., He W., Hu W., Xu Y., Chen J., Wu C., Jiang J. Prognostic role of tumor-infiltrating lymphocytes in lung cancer: A meta-analysis.
Cellular Physiology and Biochemistry 2015;37:1560-71.
- Ghani K., Cottin S., Kamen A., Caruso M. Generation of a high-titer packaging cell line for the production of retroviral vectors in suspension and serum-free media.
Gene Therapy 2007;14:1705-11.
- Gooden M. J. M., Wiersma V. R., Boerma A., Leffers N., Boezen H. M., ten Hoor K. A., Hollema H., Walenkamp A. M. E., Daemen T., Nijman H. W., Bremer E. Elevated serum CXCL16 is an independent predictor of poor survival in ovarian cancer and may reflect pro-metastatic ADAM protease activity.
British Journal of Cancer 2014;110:1535-44.
- Gorbachev A. V., Kobayashi H., Kudo D., Tannenbaum C. S., Finke J. H., Shu S., Farber J. M., Fairchild R. L. CXC chemokine ligand 9/monokine induced by IFN- γ production by tumor cells is critical for T cell-mediated suppression of cutaneous tumors.
The Journal of Immunology 2007;178:2278-86.
- Gorelik L., Flavell R. A. Immune-mediated eradication of tumors through the blockade of transforming growth factor- β signaling in T cells.
Nature Medicine 2001;7:1118-22.
- Grada Z., Hegde M., Byrd T., Shaffer D. R., Ghazi A., Brawley V. S., Corder A., Schönfeld K., Koch J., Dotti G., Heslop H. E., Gottschalk S., Wels W. S., Baker M. L., Ahmed N. TanCAR: A novel bispecific chimeric antigen receptor for cancer immunotherapy.
Molecular Therapy Nucleic Acids 2013;2:e105.
- Günther C., Carballido-Perrig N., Kaesler S., Carballido J. M., Biedermann T. CXCL16 and CXCR6 are upregulated in psoriasis and mediate cutaneous recruitment of human CD8⁺ T cells.
Journal of Investigative Dermatology 2012;132:626-34.
- Gutwein P., Schramme A., Sinke N., Abdel-Bakky M. S., Voss B., Obermüller N., Doberstein K., Koziolok M., Fritzsche F., Johannsen M., Jung K., Schaidt H., Altevogt P., Ludwig A., Pfeilschifter J., Kristiansen G. Tumoural CXCL16 expression is a novel prognostic marker of longer survival times in renal cell cancer patients.
European Journal of Cancer 2009;45:478-89.
- Ha H. K., Lee W., Park H. J., Lee S. D., Lee J. Z., Chung M. K. Clinical significance of CXCL16/CXCR6 expression in patients with prostate cancer.
Molecular Medicine Reports 2011;4:419-24.
- Hald S. M., Kiselev Y., Al-Saad S., Richardsen E., Johannessen C., Eilertsen M., Kilvaer T. K., Al-Shibli K., Andersen S., Busund L.-T., Bremnes R. M., Donnem T. Prognostic impact of CXCL16 and CXCR6 in non-small cell lung cancer: Combined high CXCL16 expression in tumor stroma and cancer cells yields improved survival.
BMC Cancer 2015;15:441.
- Hanahan D., Coussens Lisa M. Accessories to the crime: Functions of cells recruited to the tumor microenvironment.
Cancer Cell 2012;21:309-22.

- Hanahan D., Weinberg Robert A. Hallmarks of cancer: The next generation.
Cell 2011;144:646-74.
- Hanenberg H., Xiao X. L., Dilloo D., Hashino K., Kato I., Williams D. A. Colocalization of retrovirus and target cells on specific fibronectin fragments increases genetic transduction of mammalian cells.
Nature Medicine 1996;2:876-82.
- Hara T., Katakai T., Lee J.-H., Nambu Y., Nakajima-Nagata N., Gonda H., Sugai M., Shimizu A. A transmembrane chemokine, CXC chemokine ligand 16, expressed by lymph node fibroblastic reticular cells has the potential to regulate T cell migration and adhesion.
International Immunology 2006;18:301-11.
- Harlin H., Meng Y., Peterson A. C., Zha Y., Tretiakova M., Slingluff C., McKee M., Gajewski T. F. Chemokine expression in melanoma metastases associated with CD8 T-cell recruitment.
Cancer Research 2009;69:3077-85.
- Hattermann K., Ludwig A., Gieselmann V., Held-Feindt J., Mentlein R. The chemokine CXCL16 induces migration and invasion of glial precursor cells via its receptor CXCR6.
Molecular and Cellular Neuroscience 2008;39:133-41.
- Herter J., Zarbock A. Integrin regulation during leukocyte recruitment.
The Journal of Immunology 2013;190:4451-57.
- Heydtmann M., Lalor P. F., Eksteen J. A., Hübscher S. G., Briskin M., Adams D. H. CXC chemokine ligand 16 promotes integrin-mediated adhesion of liver-infiltrating lymphocytes to cholangiocytes and hepatocytes within the inflamed human liver.
The Journal of Immunology 2005;174:1055-62.
- Hojo S., Koizumi K., Tsuneyama K., Arita Y., Cui Z., Shinohara K., Minami T., Hashimoto I., Nakayama T., Sakurai H., Takano Y., Yoshie O., Tsukada K., Saiki I. High-level expression of chemokine CXCL16 by tumor cells correlates with a good prognosis and increased tumor-infiltrating lymphocytes in colorectal cancer.
Cancer Research 2007;67:4725-31.
- Hombach A. A., Abken H. Of chimeric antigen receptors and antibodies: OX40 and 41BB costimulation sharpen up T cell-based immunotherapy of cancer.
Immunotherapy 2013;5:677-81.
- Homey B., Müller A., Zlotnik A. Chemokines: Agents for the immunotherapy of cancer?
Nature Reviews Immunology 2002;2:175-84.
- Hong M., Paux A.-L., Huang C., Loumagne L., Tow C., Mackay C., Kato M., Prévost-Blondel A., Avril M.-F., Nardin A., Abastado J.-P. Chemotherapy induces intratumoral expression of chemokines in cutaneous melanoma, favoring T-cell infiltration and tumor control.
Cancer Research 2011;71:6997-7009.
- Hoyos V., Savoldo B., Quintarelli C., Mahendravada A., Zhang M., Vera J., Heslop H. E., Rooney C. M., Brenner M. K., Dotti G. Engineering CD19-specific T lymphocytes with interleukin-15 and a suicide gene to enhance their anti-lymphoma/leukemia effects and safety.
Leukemia 2010;24:1160-70.

Iwamura T., Katsuki T., Ide K. Establishment and characterization of a human pancreatic cancer cell line (SUIT-2) producing carcinoembryonic antigen and carbohydrate antigen 19-9.

Japanese Journal of Cancer Research GANN 1987;78:54-62.

Jacobs C., Duewell P., Heckelsmiller K., Wei J., Bauernfeind F., Ellermeier J., Kisser U., Bauer C. A., Dauer M., Eigler A., Maraskovsky E., Endres S., Schnurr M. An ISCOM vaccine combined with a TLR9 agonist breaks immune evasion mediated by regulatory T cells in an orthotopic model of pancreatic carcinoma.

International Journal of Cancer 2011;128:897-907.

Joyce J. A., Pollard J. W. Microenvironmental regulation of metastasis.

Nature Reviews Cancer 2009;9:239-52.

June C. H. Adoptive T cell therapy for cancer in the clinic.

Journal of Clinical Investigation 2007;117:1466-76.

Kalos M., June C. H. Adoptive T cell transfer for cancer immunotherapy in the era of synthetic biology.

Immunity 2013;39:49-60.

Ke C., Ren Y., Lv L., Hu W., Zhou W. Association between CXCL16/CXCR6 expression and the clinicopathological features of patients with non-small cell lung cancer.

Oncology Letters 2017;13:4661-68.

Keeley E. C., Mehrad B., Strieter R. M. Chemokines as mediators of tumor angiogenesis and neovascularization.

Experimental Cell Research 2011;317:685-90.

Kershaw M. H., Westwood J. A., Parker L. L., Wang G., Eshhar Z., Mavroukakis S. A., White D. E., Wunderlich J. R., Canevari S., Rogers-Freezer L., Chen C. C., Yang J. C., Rosenberg S. A., Hwu P. A phase I study on adoptive immunotherapy using gene-modified T cells for ovarian cancer.

Clinical Cancer Research 2006;12:6106-15.

Kobold S., Grassmann S., Chaloupka M., Lampert C., Wenk S., Kraus F., Rapp M., Düwell P., Zeng Y., Schmollinger J. C., Schnurr M., Endres S., Rothenfuß S. Impact of a new fusion receptor on PD-1-mediated immunosuppression in adoptive T cell therapy.

Journal of the National Cancer Institute 2015;107:djv146.

Lee J. T., Lee S. D., Lee J. Z., Chung M. K., Ha H. K. Expression analysis and clinical significance of CXCL16/CXCR6 in patients with bladder cancer.

Oncology Letters 2013;5:229-35.

Lehrke M., Millington S. C., Lefterova M., Cumarantunge R. G., Szapary P., Wilensky R., Rader D. J., Lazar M. A., Reilly M. P. CXCL16 is a marker of inflammation, atherosclerosis, and acute coronary syndromes in humans.

Journal of the American College of Cardiology 2007;49:442-49.

Liang K., Liu Y., Eer D., Liu J., Yang F., Hu K. High CXC chemokine ligand 16 (CXCL16) expression promotes proliferation and metastasis of lung cancer via regulating the NF- κ B pathway.

International Medical Journal of Experimental and Clinical Research 2018;24:405-11.

- Liao D., Luo Y., Markowitz D., Xiang R., Reisfeld R. A. Cancer associated fibroblasts promote tumor growth and metastasis by modulating the tumor immune microenvironment in a 4T1 murine breast cancer model.
PLoS One 2009;4:e7965.
- Lim W. A., June C. H. The principles of engineering immune cells to treat cancer.
Cell 2017;168:724-40.
- Liu X., Ranganathan R., Jiang S., Fang C., Sun J., Kim S., Newick K., Lo A., June C. H., Zhao Y., Moon E. K. A chimeric switch-receptor targeting PD1 augments the efficacy of second-generation CAR T cells in advanced solid tumors.
Cancer Research 2016;76:1578-90.
- Lonez C., Verma B., Hendlisz A., Aftimos P., Awada A., Van Den Neste E., Catala G., Machiels J.-P. H., Piette F., Brayer J. B., Sallman D. A., Kerre T., Odunsi K., Davila M. L., Gilham D. E., Lehmann F. F. Study protocol for THINK: A multinational open-label phase I study to assess the safety and clinical activity of multiple administrations of NKR-2 in patients with different metastatic tumour types.
BMJ Open 2017;7:e017075.
- Lugade A. A., Sorensen E. W., Gerber S. A., Moran J. P., Frelinger J. G., Lord E. M. Radiation-induced IFN- γ production within the tumor microenvironment influences antitumor immunity.
The Journal of Immunology 2008;180:3132-39.
- Mackay C., Marston W., Dudler L. Naive and memory T cells show distinct pathways of lymphocyte recirculation.
The Journal of Experimental Medicine 1990;171:801-17.
- Matloubian M., David A., Engel S., Ryan J. E., Cyster J. G. A transmembrane CXC chemokine is a ligand for HIV-coreceptor Bonzo.
Nature Immunology 2000;1:298-304.
- Matsumura S., Wang B., Kawashima N., Braunstein S., Badura M., Cameron T. O., Babb J. S., Schneider R. J., Formenti S. C., Dustin M. L., Demaria S. Radiation-induced CXCL16 release by breast cancer cells attracts effector T cells.
The Journal of Immunology 2008;181:3099-107.
- Meijer J., Ogink J., Kreike B., Nuyten D., de Visser K. E., Roos E. The chemokine receptor CXCR6 and its ligand CXCL16 are expressed in carcinomas and inhibit proliferation.
Cancer Research 2008;68:4701-08.
- Mittal D., Gubin M. M., Schreiber R. D., Smyth M. J. New insights into cancer immunoediting and its three component phases — elimination, equilibrium and escape.
Current Opinion in Immunology 2014;27:16-25.
- Molon B., Gri G., Bettella M., Gómez-Moutón C., Lanzavecchia A., Martínez-A C., Mañes S., Viola A. T cell costimulation by chemokine receptors.
Nature Immunology 2005;6:465-71.
- Moon E. K., Carpenito C., Sun J., Wang L.-C. S., Kapoor V., Predina J., Powell D. J., Riley J. L., June C. H., Albelda S. M. Expression of a functional CCR2 receptor enhances tumor localization and tumor eradication by retargeted human T cells expressing a mesothelin - specific chimeric antibody receptor.
Clinical Cancer Research 2011;17:4719-30.

- Morgan R. A., Johnson L. A., Davis J. L., Zheng Z., Woolard K. D., Reap E. A., Feldman S. A., Chinnasamy N., Kuan C.-T., Song H., Zhang W., Fine H. A., Rosenberg S. A. Recognition of glioma stem cells by genetically modified T cells targeting EGFRvIII and development of adoptive cell therapy for glioma.
Human Gene Therapy 2012;23:1043-53.
- Morgan R. A., Yang J. C., Kitano M., Dudley M. E., Laurencot C. M., Rosenberg S. A. Case report of a serious adverse event following the administration of T cells transduced with a chimeric antigen receptor recognizing ERBB2.
Molecular Therapy 2010;18:843-51.
- Morita S., Kojima T., Kitamura T. Plat-E: An efficient and stable system for transient packaging of retroviruses.
Gene Therapy 2000;7:1063-66.
- Müller A., Homey B., Soto H., Ge N., Catron D., Buchanan M. E., McClanahan T., Murphy E., Yuan W., Wagner S. N., Barrera J. L., Mohar A., Verástegui E., Zlotnik A. Involvement of chemokine receptors in breast cancer metastasis.
Nature 2001;410:50-6.
- Müller N., Michen S., Tietze S., Töpfer K., Schulte A., Lamszus K., Schmitz M., Schackert G., Pastan I., Temme A. Engineering NK cells modified with an EGFRvIII-specific chimeric antigen receptor to overexpress CXCR4 improves immunotherapy of CXCL12/SDF-1 α -secreting glioblastoma.
Journal of Immunotherapy 2015;38:197-210.
- Musha H., Ohtani H., Mizoi T., Kinouchi M., Nakayama T., Shiiba K., Miyagawa K., Nagura H., Yoshie O., Sasaki I. Selective infiltration of CCR5+CXCR3+ T lymphocytes in human colorectal carcinoma.
International Journal of Cancer 2005;116:949-56.
- Nakayama T., Hieshima K., Izawa D., Tatsumi Y., Kanamaru A., Yoshie O. Cutting edge: Profile of chemokine receptor expression on human plasma cells accounts for their efficient recruitment to target tissues.
The Journal of Immunology 2003;170:1136-40.
- Nandi A., Estess P., Siegelman M. Bimolecular complex between rolling and firm adhesion receptors required for cell arrest: CD44 association with VLA-4 in T cell extravasation.
Immunity 2004;20:455-65.
- Neel N. F., Schutyser E., Sai J., Fan G.-H., Richmond A. Chemokine receptor internalization and intracellular trafficking.
Cytokine & Growth Factor Reviews 2005;16:637-58.
- Oh S.-T., Schramme A., Tilgen W., Gutwein P., Reichrath J. Overexpression of CXCL16 in lesional psoriatic skin.
Dermato-Endocrinology 2009;1:114-18.
- Ohta M., Tanaka F., Yamaguchi H., Sadanaga N., Inoue H., Mori M. The high expression of Fractalkine results in a better prognosis for colorectal cancer patients.
International Journal of Oncology 2005;26:41-7.
- Pardoll D. M. The blockade of immune checkpoints in cancer immunotherapy.
Nature Reviews Cancer 2012;12:252-64.

- Park J. H., Geyer M. B., Brentjens R. J. CD19-targeted CAR T-cell therapeutics for hematologic malignancies: Interpreting clinical outcomes to date. *Blood* 2016;127:3312-20.
- Peng W., Ye Y., Rabinovich B. A., Liu C., Lou Y., Zhang M., Whittington M., Yang Y., Overwijk W. W., Lizée G., Hwu P. Transduction of tumor-specific T cells with CXCR2 chemokine receptor improves migration to tumor and antitumor immune responses. *Clinical Cancer Research* 2010;16:5458-68.
- Porter D., Frey N., Wood P. A., Weng Y., Grupp S. A. Grading of cytokine release syndrome associated with the CAR T cell therapy tisagenlecleucel. *Journal of Hematology & Oncology* 2018;11:35.
- Prapa M., Caldrea S., Spano C., Bestagno M., Golinelli G., Grisendi G., Petrachi T., Conte P., Horwitz E. M., Campana D., Paolucci P., Dominici M. A novel anti-GD2/4-1BB chimeric antigen receptor triggers neuroblastoma cell killing. *Oncotarget* 2015;6:24884-94.
- Rabinovich G. A., Gabrilovich D., Sotomayor E. M. Immunosuppressive strategies that are mediated by tumor cells. *Annual Review of Immunology* 2007;25:267-96.
- Raman D., Baugher P. J., Thu Y. M., Richmond A. Role of chemokines in tumor growth. *Cancer Letters* 2007;256:137-65.
- Raman D., Sobolik-Delmaire T., Richmond A. Chemokines in health and disease. *Experimental Cell Research* 2011;317:575-89.
- Ran F. A., Hsu P. D., Wright J., Agarwala V., Scott D. A., Zhang F. Genome engineering using the CRISPR-Cas9 system. *Nature Protocols* 2013;8:2281-308.
- Rapp M., Grassmann S., Chaloupka M., Layritz P., Kruger S., Ormanns S., Rataj F., Janssen K.-P., Endres S., Anz D., Kobold S. C-C chemokine receptor type-4 transduction of T cells enhances interaction with dendritic cells, tumor infiltration and therapeutic efficacy of adoptive T cell transfer. *Oncoimmunology* 2016;5:e1105428.
- Rataj F., Kraus F. B. T., Chaloupka M., Grassmann S., Heise C., Cadilha B. L., Duewell P., Endres S., Kobold S. PD1-CD28 fusion protein enables CD4+ T cell help for adoptive T cell therapy in models of pancreatic cancer and Non-Hodgkin lymphoma. *Frontiers in Immunology* 2018;9.
- Restifo N. P., Dudley M. E., Rosenberg S. A. Adoptive immunotherapy for cancer: Harnessing the T cell response. *Nature Reviews Immunology* 2012;12:269-81.
- Rosenberg S. A., Dudley M. E. Cancer regression in patients with metastatic melanoma after the transfer of autologous antitumor lymphocytes. *Proceedings of the National Academy of Sciences of the United States of America* 2004a;101:14639-45.
- Rosenberg S. A., Sherry R. M., Morton K. E., Scharfman W. J., Yang J. C., Topalian S. L., Royal R. E., Kammula U., Restifo N. P., Hughes M. S., Schwartzentruber D., Berman D. M., Schwarz S. L., Ngo L. T., Mavroukakis S. A., White D. E., Steinberg S. M. Tumor progression

can occur despite the induction of very high levels of self/tumor antigen-specific CD8 T cells in patients with melanoma.

The Journal of Immunology 2005;175:6169-76.

Rosenberg S. A., Yang J. C., Restifo N. P. Cancer immunotherapy: Moving beyond current vaccines.

Nature Medicine 2004b;10:909-15.

Rühland S., Wechselberger A., Spitzweg C., Huss R., Nelson P. J., Harz H. Quantification of in vitro mesenchymal stem cell invasion into tumor spheroids using selective plane illumination microscopy.

Journal of Biomedical Optics 2015;20:3.

Schaer D. A., Lesokhin A. M., Wolchok J. D. Hiding the road signs that lead to tumor immunity.

The Journal of Experimental Medicine 2011;208:1937-40.

Schmohl K. A., Müller A. M., Wechselberger A., Rühland S., Salb N., Schwenk N., Heuer H., Carlsen J., Göke B., Nelson P. J., Spitzweg C. Thyroid hormones and tetrac: New regulators of tumour stroma formation via integrin $\alpha\beta 3$.

Endocrine-Related Cancer 2015;22:941-52.

Schramme A., Abdel-Bakky M. S., Kämpfer-Kolb N., Pfeilschifter J., Gutwein P. The role of CXCL16 and its processing metalloproteinases ADAM10 and ADAM17 in the proliferation and migration of human mesangial cells.

Biochemical and Biophysical Research Communications 2008;370:311-16.

Siddiqui I., Erreni M., van Brakel M., Debets R., Allavena P. Enhanced recruitment of genetically modified CX3CR1-positive human T cells into Fractalkine/CX3CL1 expressing tumors: Importance of the chemokine gradient.

Journal for Immunotherapy of Cancer 2016;4:21.

Singbartl K. A. I., Forlow S. B., Ley K. Platelet, but not endothelial, P-selectin is critical for neutrophil-mediated acute postischemic renal failure.

The FASEB Journal 2001;15:2337-44.

Singh S. K., Mishra M. K., Eltoun I.-E. A., Bae S., Lillard J. W., Singh R. CCR5/CCL5 axis interaction promotes migratory and invasiveness of pancreatic cancer cells.

Scientific Reports 2018;8:1323.

Smith M. C. P., Luker K. E., Garbow J. R., Prior J. L., Jackson E., Piwnica-Worms D., Luker G. D. CXCR4 regulates growth of both primary and metastatic breast cancer.

Cancer Research 2004;64:8604-12.

Soria G., Ofri-Shahak M., Haas I., Yaal-Hahoshen N., Leider-Trejo L., Leibovich-Rivkin T., Weitzenfeld P., Meshel T., Shabtai E., Gutman M., Ben-Baruch A. Inflammatory mediators in breast cancer: Coordinated expression of TNF α & IL-1 β with CCL2 & CCL5 and effects on epithelial-to-mesenchymal transition.

BMC Cancer 2011;11:130-.

Stancovski I., Schindler D. G., Waks T., Yarden Y., Sela M., Eshhar Z. Targeting of T lymphocytes to Neu/HER2-expressing cells using chimeric single chain Fv receptors.

The Journal of Immunology 1993;151:6577-82.

Stein J. V., Nombela-Arrieta C. Chemokine control of lymphocyte trafficking: A general overview.

Immunology 2005;116:1-12.

Tabata S., Kadowaki N., Kitawaki T., Shimaoka T., Yonehara S., Yoshie O., Uchiyama T. Distribution and kinetics of SR-PSOX/CXCL16 and CXCR6 expression on human dendritic cell subsets and CD4⁺ T cells.

Journal of Leukocyte Biology 2005;77:777-86.

Topalian S. L., Sznol M., McDermott D. F., Kluger H. M., Carvajal R. D., Sharfman W. H., Brahmer J. R., Lawrence D. P., Atkins M. B., Powderly J. D., Leming P. D., Lipson E. J., Puzanov I., Smith D. C., Taube J. M., Wigginton J. M., Kollia G. D., Gupta A., Pardoll D. M., Sosman J. A., Hodi F. S. Survival, durable tumor remission, and long-term safety in patients with advanced melanoma receiving nivolumab.

Journal of Clinical Oncology 2014;32:1020-30.

Unutmaz D., Xiang W., Sunshine M. J., Campbell J., Butcher E., Littman D. R. The primate lentiviral receptor Bonzo/STRL33 is coordinately regulated with CCR5 and its expression pattern is conserved between human and mouse.

The Journal of Immunology 2000;165:3284-92.

Wang J., Jensen M., Lin Y., Sui X., Chen E., Lindgren C. G., Till B., Raubitschek A., Forman S. J., Qian X., James S., Greenberg P., Riddell S., Press O. W. Optimizing adoptive polyclonal T cell immunotherapy of lymphomas, using a chimeric T cell receptor possessing CD28 and CD137 costimulatory domains.

Human Gene Therapy 2007;18:712-25.

Wang M., Yin B., Wang H. Y., Wang R.-F. Current advances in T-cell-based cancer immunotherapy.

Immunotherapy 2014;6:1265-78.

Wente M., Gaida M., Mayer C. Expression and potential function of the CXC chemokine CXCL16 in pancreatic ductal adenocarcinoma.

International Journal of Oncology 1992:297-308.

Wilbanks A., Zondlo S. C., Murphy K., Mak S., Soler D., Langdon P., Andrew D. P., Wu L., Briskin M. Expression cloning of the STRL33/BONZO/TYMSTR ligand reveals elements of CC, CXC, and CX3C chemokines.

The Journal of Immunology 2001;166:5145-54.

Yang X., Chu Y., Wang Y., Zhang R., Xiong S. Targeted in vivo expression of IFN- γ -inducible protein 10 induces specific antitumor activity.

Journal of Leukocyte Biology 2006;80:1434-44.

Zhang J., Lu Y., Pienta K. J. Multiple roles of chemokine (C-C Motif) ligand 2 in promoting prostate cancer growth.

Journal of the National Cancer Institute 2010;102:522-28.

Zhang L., Conejo-Garcia J. R., Katsaros D., Gimotty P. A., Massobrio M., Regnani G., Makrigiannakis A., Gray H., Schlienger K., Liebman M. N., Rubin S. C., Coukos G. Intratumoral T cells, recurrence, and survival in epithelial ovarian cancer.

New England Journal of Medicine 2003;348:203-13.

Zhang L., Ran L., Garcia G. E., Wang X. H., Han S., Du J., Mitch W. E. Chemokine CXCL16 regulates neutrophil and macrophage infiltration into injured muscle, promoting muscle regeneration.

The American Journal of Pathology 2009;175:2518-27.

Reference list

Zhu Y. M., Webster S. J., Flower D., Woll P. J. Interleukin-8/CXCL8 is a growth factor for human lung cancer cells.

British Journal of Cancer 2004;91:1970-76.

Zlotnik A., Yoshie O. Chemokines.

Immunity 2000;12:121-27.

8 Appendices

8.1 Abbreviations

ACT	Adoptive cell therapy
ADAM	A disintegrin and metalloprotease
ATCC	American Type Culture Collection
BSA	Bovine serum albumin
CAR	Chimeric antigen receptor
CD	Cluster of differentiation
CTLA-4	Cytotoxic T lymphocyte-associated antigen 4
Cy	Cyanine
DMEM	Dulbecco's modified Eagle's medium
DMSO	Dimethyl sulfoxide
DNA	Deoxyribonucleic acid
EGFRvIII	Epidermal growth factor receptor variant III
ELISA	Enzyme-linked immunosorbent assay
FACS	Fluorescence-activated cell sorting
FCS	Fetal calf serum
FDA	U.S. Food and Drug Administration
FITC	Fluorescein isothiocyanate
GFP	Green fluorescent protein
HLA	Human leukocyte antigen
IFN-γ	Interferon- γ
IL	Interleukin
i.v.	Intravenous
LNi	Ipsilateral lymph node
LNc	Contralateral lymph node
MDSC	Myeloid-derived suppressor cell

n.d.	Not detectable
NEAA	Non-essential amino acids
NK cell	Natural killer cell
OVA	Ovalbumin
qRT-PCR	Quantitative real-time PCR
PD-1	Programmed cell death protein 1
PD-L1	Programmed cell death ligand 1
PBMC	Peripheral blood mononuclear cell
PBS	Phosphate-buffered saline
PE	Phycoerythrin
PerCP	Peridinin chlorophyll protein complex
RNA	Ribonucleic acid
RPMI	Roswell Park Memorial Institute
s.c.	Subcutaneous
scFv	Single chain variable fragment
SEM	Standard error of mean
STR	Short tandem repeats
TAA	Tumor-associated antigen
TAM	Tumor-associated macrophage
TCR	T cell receptor
TGF-β	Transforming growth factor- β
TIL	Tumor-infiltrating lymphocyte
TME	Tumor microenvironment
Treg cell	Regulatory T cell
VLE	Very low endotoxin
WHO	World Health Organization

8.2 Publications

S. Stoiber, BL. Cadilha, MR. Benmebarek, **S. Lesch**, S. Endres, S. Kobold. Limitations in the design of chimeric antigen receptors for cancer therapy. *Cells* 2019, 8(5), 472. Review.

MR. Benmebarek, C. Karches, B. Cadilha, **S. Lesch**, S. Endres, S. Kobold. Killing mechanisms of chimeric antigen receptor (CAR) T cells. *Int. J. Mol. Sci.* 2019, 20(6). Review.

S. Kailayangiri, B. Altvater, **S. Lesch**, S. Balbach, C. Göttlich, J. Kuehnemundt, JH. Mikesch, S. Schellhaas, S. Jamitzky, J. Meltzer, N. Farwick, L. Greune, M. Fluegge, K.Kerl, H. Lode, N. Siebert, I. Muller, H. Walles, W. Hartmann, C. Rossig. EZH2 inhibition in Ewing sarcoma upregulates GD2 expression for targeting with gene-modified T cells. *Mol Ther.* 2019, 27(5).

Eidesstattliche Versicherung

Lesch, Stefanie

Name, Vorname

Ich erkläre hiermit an Eides statt,
dass ich die vorliegende Dissertation mit dem Thema

Engineering model antigen-specific T cells to overexpress the chemokine receptor CXCR6 improves homing of adoptively transferred T cells in subcutaneous tumor models

selbständig verfasst, mich außer der angegebenen keiner weiteren Hilfsmittel bedient und alle Erkenntnisse, die aus dem Schrifttum ganz oder annähernd übernommen sind, als solche kenntlich gemacht und nach ihrer Herkunft unter Bezeichnung der Fundstelle einzeln nachgewiesen habe.

Ich erkläre des Weiteren, dass die hier vorgelegte Dissertation nicht in gleicher oder in ähnlicher Form bei einer anderen Stelle zur Erlangung eines akademischen Grades eingereicht wurde.

München, 29.10.2019

Ort, Datum

Stefanie Lesch

Unterschrift Doktorandin/Doktorand